MARTIN MARIETTA ENERGY SYSTEMS LIBRARIES
3 4456 0360671 0

CENTRAL RESEARCH LIBRARY
DOCUMENT COLLECTION

ORNL-1599
Physics
Cy. 5

MAGNETIC SUSCEPTIBILITY OF ANNEALED AND FAST-NEUTRON BOMBARDED GERMANIUM

D. K. Stevens

CENTRAL RESEARCH LIBRARY
DOCUMENT COLLECTION

LIBRARY LOAN COPY

DO NOT TRANSFER TO ANOTHER PERSON

If you wish someone else to see this document, send in name with document and the library will arrange a loan.

OAK RIDGE NATIONAL LABORATORY
OPERATED BY
CARBIDE AND CARBON CHEMICALS COMPANY
A DIVISION OF UNION CARBIDE AND CARBON CORPORATION
UCC
POST OFFICE BOX P
OAK RIDGE, TENNESSEE

ORNL 1599
Copy No 5

Contract No W 7405 eng 26

MAGNETIC SUSCEPTIBILITY OF ANNEALED AND FAST NEUTRON BOMBARDED GERMANIUM

D K Stevens

DATE ISSUED

SEP 17 1954

OAK RIDGE NATIONAL LABORATORY
Operated by
CARBIDE AND CARBON CHEMICALS COMPANY
A Division of Union Ca bide and Ca bon Co poration
Post Office Box P
Oak Ridge Tennessee

3 4456 0360671 0

INTERNAL DISTRIBUTION

1 C E Center
2 Biology Library
3 Health Physics Library
4 5 Central Research Library
6 Reactor Experimental Engineering Library
7 11 Laboratory Records Department
12 Laboratory Records ORNL R C
13 C E Larson
14 L B Emlet (K 25)
15 J P Murray (Y 12)
16 A M Weinberg
17 E H Taylor
18 E D Shipley
19 D S Billington
20 F C VonderLage
21 R C Briant
22 C P Keim
23 J A Lane
24 J H Frye Jr
25 R S Livingston
26 J A Swartout
27 S C Lind
28 F L Culler
29 A H Snell
30 A Hollaender
31 M T Kelley
32 G H Clewett
33 K Z Morgan
34 T A Lincoln
35 A S Householder
36 C S Harrill
37 C E Winters
38 D W Cardwell
39 E M King
40 A J Miller
41 D D Cowen
42 P M Reyling
43 G C Williams
44 58 D K Stevens

EXTERNAL DISTRIBUTION

59 R F Bacher California Institute of Technology
60 R L Sproull Physics Department Cornell University
61 J I Budnick Physics Department Rutgers University
62 E I Salkovitz Naval Research Laboratory
63 C J Kriessman Remington Rand Corporation Philadelphia
64 83 H D Crockford Chemistry Department University of North Carolina
84 133 Oak Ridge Institute of Nuclear Studies
134 391 Given distribution as shown in TID 4500 under Physics Category

DISTRIBUTION PAGE TO BE REMOVED IF REPORT IS GIVEN PUBLIC DISTRIBUTION

This research was conducted at the Oak Ridge National Laboratory under an Oak Ridge Institute of Nuclear Studies Fellowship The author who is a student at the University of North Carolina a member university of the Oak Ridge Institute of Nuclear Studies is deeply mindful of the cooperative effort between the Institute the Laboratory and the Office of the Dean of the Graduate School of the University The author is grateful to the Institute and the Laboratory for making this work possible and is especially indebted to the University Relations Division of the Institute for its generous assistance The personnel of the Laboratory have been most cooperative and helpful

ACKNOWLEDGMENTS

The author wishes to express his deep appreciation to J H Crawford Jr Assistant Director of the Solid State Division of the Oak Ridge National Laboratory for suggesting the problem and for his keen interest and guidance throughout the course of the work The active interest and many helpful suggestions offered by D S Billington Director of the Solid State Division and second member of the author s local committee are also gratefully acknowledged The author appreciates the efforts of J C Pigg for his design and development of a magnet field control device of sufficient sensitivity for this problem J W Cleland for his measurements of the Hall coefficient and conductivity of the companion crystals and his assistance in conducting the irradiations Miss Louise Roth of the Physics Department of Purdue University for preparing the samples and R L Sproull of the Physics Department of Cornell University for suggesting the balance detector circuit The author is also mindful of the efforts of J T Howe and W E Busby for their work in preparing the drawings and plots of data Mary LaMaster and Gladys Warren for typing the dissertation and R J Fox of the Research Shops for his part in supervising the construction of the balance and cryostat

The author is particularly grateful to his university advisor Professor H D Crockford of the Chemistry Department of the University of North Carolina for his unceasing efforts on behalf of this research project and his unselfish gift of time in making numerous trips from Chapel Hill to Oak Ridge

MAGNETIC SUSCEPTIBILITY OF ANNEALED AND FAST-NEUTRON BOMBARDED GERMANIUM

D K Stevens

CHAPTER 1 INTRODUCTION

1 STATEMENT OF THE PROBLEM

This research is concerned with the magnetic susceptibility of single crystals of germanium with known electrical properties after having been annealed and after having undergone radiation damage as the result of fast neutron bombardment The bombardment was effected by exposure in the ORNL graphite reactor Although measurements had been made previously on unirradiated samples they were carried out on polycrystalline material of unknown impurity content and were therefore of little value in this work Information on the magnetic properties of electrons subjected to the periodic potential of the lattice and of electrons trapped in energy levels associated with fast particle produced lattice disorder was sought this information being of interest in the study of the fundamental nature of the solid state as well as in the study of radiation damage

2 THE NATURE OF RADIATION DAMAGE

The study of radiation damage that is the effects produced when crystalline bodies are exposed to highly energetic nuclear particles is a comparatively new field of scientific research being a result of the successful development of nuclear chain reactors That considerable lattice disorder with a resultant change in properties of the crystalline body might be produced was first predicted by Wigner[39] in the early days of the Manhattan Project and at one time was known as Wigner Disease Subsequently these predictions were proved correct and extensive research is being conducted in the field The result has been the accumulation of information of great interest to nuclear scientists and engineers and research in the field of solid state physics as a whole has been stimulated

See Bibliography

When a high speed massive particle (electron proton alpha particle or fission fragment) is slowed down in passing through a crystalline solid its energy is dissipated by interaction with atoms of the lattice Charged particles may lose energy in two ways (1) inelastic collisions resulting from coulombic interaction that produce excitation and ionization of the lattice atoms and (2) elastic or billard ball collisions with atomic cores For uncharged neutrons only elastic collisions are possible The energy transferred to an atom by a fast particle in an elastic collision may be sufficient to knock the atom into an interstitial lattice site some distance away from its original position Hence both a lattice vacancy and an interstitial atom are created This primary knock on in traveling through the crystal may also displace other atoms from their positions In addition if its velocity is sufficiently great the primary atom may lose energy by the inelastic process Energy loss by this process is unimportant in the case of germanium because of its relatively large atomic mass compared with the mass of a neutron The original particle and the primary and secondary knock ons may continue to produce lattice disorder until their energies are degraded to the extent that they can no longer transfer the threshold energy necessary for atomic displacement This threshold energy is 31 ev for germanium [25] The remaining energy of the particle is then lost by causing thermal agitations Seitz[39] and Slater[42] have treated the subject as a whole while Lark Horovitz[25] has calculated the number of displaced atoms in germanium and silicon by using an elementary method

The disordered regions produced by bombarding particles are submicroscopic in size This disorder is discernible by the alteration of the physical properties which are sensitive to the structure of the material In metals and alloys the plastic and electrical properties are changed [3 5 28] Observations of changes in the density and x ray

patterns of covalent crystals, such as silicon dioxide [54] and in the electrical properties of ionic crystals[30] have been made Fast neutron bombardment has been found to increase the rate of microdiffusion in some systems[4 10] in which solid state reactions may occur

The electrical properties of certain semiconductors, namely, silicon,[25] germanium,[11 25] and cuprous oxide,[36] have been found to be particularly sensitive to radiation damage After an exposure in the reactor of only a few hours the electrical conductivity of some samples has been found to change by several orders of magnitude The relatively great sensitivity of the electrical properties of this class of materials to lattice disorder makes these materials particularly useful in the study of radiation effects in solids

3 THE NATURE OF SEMICONDUCTORS

Semiconductors may be defined as that class of materials in which thermal energy is required to release charge carriers for the conduction of electrical current These charge carriers may arise from two distinct sources (1) the undistorted host lattice and (2) ionizable impurities and lattice defects Removal of an electron from a covalent bond and the removal of an electron from a negative ion are examples of the first case which gives rise to intrinsic conduction In this process two charge carriers are produced an ionized electron and a vacant electronic state a hole which is mobile by virtue of the interchange of electrons from equivalent occupied states The second source of current carriers gives rise to impurity or extrinsic conduction and only one carrier is produced

The types of ionizable defects or impurity atoms which give rise to conduction vary in nature with the chemical constitution of the particular semiconductor in question In the case of ionic semiconductors such as zinc oxide cuprous oxide or lead sulfide the ionizable impurity is usually a stoichiometric excess of one of the constituent elements If the electropositive element is in excess as in zinc oxide the impurities give up electrons and are called donors In the case of cuprous oxide the electronegative component is in excess Upon ionization an electron is accepted and hole conduction takes place These impurities are called acceptors Electron conductors are called *n* type semiconductors and hole conductors are termed *p* type Lead sulfide may be either an *n*-type or a *p* type conductor[18] as a result of previous chemical treatment

Impurities in silicon and germanium are of a quite different nature In these covalent crystals of the diamond form an impurity atom from the fifth column of the periodic table when occupying a normal lattice site supplies one electron in excess of the number needed to complete the four directed valence bonds associated with its position in the crystal The extra electron is loosely bound to the impurity atom by electrostatic forces and is easily ionized by thermal vibrations When on the other hand an atom from the third column of the periodic table is substituted in the lattice there is a deficiency of one electron for the completion of these four covalent bonds There is one incomplete bond localized around the impurity atom which may be detached by thermal energy and may then accept an electron from neighboring states and move through the crystal in the form of a hole

It is well known that lattice vacancies in alkali halide crystals can trap electrons released from negative ions by ionizing radiation to form color centers [27] Recently studies of controlled introduction of lattice defects by nucleon bombardment have shown conclusively that lattice defects so produced may behave as electron traps and hole traps and, in the case of germanium as acceptors Although low temperature irradiation produces exceedingly complex results in germanium so far as the nature and distribution of energy levels are concerned,[13] most of the complexity is thermally unstable at room temperature and rapidly anneals The results of irradiation at about 35°C[11] show that fast neutron disordering produces predominantly electron traps which are sufficiently low lying to act also as acceptors in *p* type material During bombardment the conductivity of originally *n* type material decreases passes through a minimum and then increases at an appreciably lower rate Just prior to passing through the minimum there is a change from *n* to *p* type material

Since the total conductivity σ is a sum of the contributions of both holes and electrons,

$$\sigma = e(n_e\mu_e + n_h\mu_h) \tag{1}$$

where e is the electronic charge μ and n are the mobility and concentration of carriers respectively and the subscripts refer to either electrons or holes The concentrations of the holes and

electrons are related by the equilibrium equation or carrier product

$$(2) \quad n_e n_h = \frac{2^2(2\pi\sqrt{m_e m_h}\,kT)^3}{h^6}\, e^{-E_g/kT}$$

where m_e and m_h are the effective carrier masses k is the Boltzmann constant h is the Planck constant E_g is the ionization energy for the intrinsic process, and T is temperature Equation 2 and the room temperature intrinsic concentration of electrons or holes in germanium being $\sim 3 \times 10^{13}$ cm^3 show that the conductivity of n type germanium with $n_e \geqq 10^{15}$ cm^{-3} is almost entirely due to electrons Consequently the acceptors introduced by bombardment remove electrons until conversion to the p type occurs after which the acceptors upon ionization produce holes This process is quite analogous both in principle and theory to the conductometric titration of an acid with a weak base

In addition it has been demonstrated that shallow hole traps are also introduced, but these are ineffective unless the concentration of holes is large or the temperature is low These traps are unimportant in n type material but are observable in high conductivity p type material

It has been postulated[25 11] that the acceptors or electron traps are associated with lattice vacancies, while the shallow traps are associated with interstitial atoms James and Lark Horovitz[22] have attempted to refine these postulates by proposing a semiquantitative model based on the modification of the ionization potentials of the valence electrons of the interstitial atoms by the dielectric constant of the germanium lattice the vacancies being treated in an analogous fashion As a result of this model, the authors postulate that there are at least six localized energy levels associated with each defect pair (interstitial vacancy pair or Frenkel defect) to accommodate the four valence electrons of the interstitial atom This model will be considered more fully in connection with the magnetic susceptibility of semiconductors Except for explaining the general features of the electrical behavior of germanium the models proposed to account for the disorder produced electronic energy levels appear to be oversimplified Consequently it was felt that information concerning the magnetic behavior of irradiated germanium would be helpful in testing the validity of the James–Lark Horovitz model

4 MAGNETIC PROPERTIES OF SEMICONDUCTORS

Upon placing a magnetically isotropic body in a magnetic field the magnetic induction B within the body is given by

$$(3) \qquad B = H + 4\pi M ,$$

where H is the field intensity and M is the intensity of magnetization or the magnetic moment per unit volume The ratio B/H is known as the permeability μ, and M/H is the magnetic susceptibility per unit volume κ The specific susceptibility is obtained by dividing κ by the density and is denoted by the symbol χ Unless specified otherwise, reference throughout will be made to the specific susceptibility

In general, according to their susceptibilities, substances may be divided into three classifications diamagnetic paramagnetic and ferromagnetic Diamagnetic materials have no magnetic moment in the absence of an external field and have a negative susceptibility which is small ($<10^{-6}$) and independent of temperature and field according to classical theory Paramagnetic and ferromagnetic substances have permanent magnetic moments and positive susceptibilities with the latter being orders of magnitude larger than the former Upon removal of the exciting field the magnetization of diamagnetic and paramagnetic bodies disappears whereas ferromagnetic bodies retain a portion of their magnetization

Diamagnetism of atoms and molecules is a consequence of the Larmor precession of the electron orbits about the direction of the exciting field and is a function only of the radius of the electronic orbits The induced magnetic moment will be of sign opposite to that of the applied field, and it represents an increase in the energy state of the atom All bodies exhibit diamagnetism but it is so weak that it is overshadowed by paramagnetic and ferromagnetic effects if they are present

Paramagnetism is due to a permanent magnetic moment of the atom or molecule and owes its origin either to the spin of unpaired electrons bound to an atom or to a resultant orbital magnetic moment of electrons Upon the application of an external field, the moments of these atoms tend to align with the field but the alignment is resisted by thermal agitation If the magnetic moment of the atom is strong enough to cause interaction with neighboring atoms ferromagnetism is exhibited

The latter is relatively uncommon in nature, where as many examples of paramagnetism are to be found particularly in the transition group elements and their compounds

Pure well annealed crystals of germanium would be expected to show no paramagnetic properties at low temperature since there are no unpaired electrons or unoccupied orbitals The magnetic susceptibility should therefore be negative and according to the classical theory be temperature independent However lattice disorder and impurity atoms having more or less than four valence atoms could have an appreciable effect on the susceptibility of these covalent crystals

Measurements of the susceptibility of germanium made prior to the current work were carried out before efficient purification procedures were developed Owen[32] conducted measurements in the temperature range −170 to 1000°C on powdered material at below its melting point χ was found to be $-0\ 30 \times 10^{-6}$ at −170°C and $-0\ 12 \times 10^{-6}$ at room temperature Stohr and Klemn[47] found susceptibilities of $-0\ 146 \times 10^{-6}$ at 183°C and $-0\ 122 \times 10^{-6}$ at room temperature Squire[45] reports a hundredfold increase in the diamagnetism of germanium at a temperature (75°K) where Cristescu and Simon[14] found a specific heat anomaly Recent measurements of the specific heat of pure germanium samples [16] however do not substantiate Cristescu and Simon s results

Except for the studies of ferromagnetic and antiferromagnetic semiconductors that is the ferrites, the only systematic study of the magnatic susceptibility of semiconductors is that of Busch and Mooser[9] on gray or alpha tin These authors divided the susceptibility into three parts (1) the contribution χ_a of the tin atoms combined in the lattice which they assumed to be temperature independent (2) the contribution χ_l due to impurity atoms or ions possessing an unpaired electron which should obey a Curie law and (3) the contribution χ_c of the free charge carriers The latter contribution consists of two components the spin paramagnetism of the carrier and the orbital diamagnetism produced by the spiral or the circular path imparted to the carrier by motion in a magnetic field

The spin component of susceptibility was first considered by Pauli[33] to explain the small temperature independent paramagnetism of the alkali metals Reasoning from band theory Pauli assumed that the band of energy levels associated with the valence electrons was split by the action of the magnetic field into two bands in one of which the electron spins were oriented parallel to the field and in the other antiparallel Since equivalent levels in the parallel orientation are lowered in energy by βH (β represents the Bohr magneton) and in the antiparallel orientation are raised by βH there will be a redistribution of the electrons favoring the parallel band This redistribution will give rise to a magnetic moment of $2\Delta n\beta$ where Δn is the increase in population of the band of parallel spins over that in the absence of the magnetic field By assuming complete degeneracy of the electron gas that is all levels completely filled up to the Fermi level and by using the classical distribution of states to determine the change in band population induced by the two fields Pauli found that the volume susceptibility due to free electrons alone is given to a good approximation by

$$\kappa = \frac{3}{2}\frac{\beta 2}{\zeta} \tag{4}$$

where ζ is the Fermi level or free energy per electron

More recently Stoner[48] treated the problem from a statistical mechanical approach His more general treatment includes not only the completely degenerate case but also the cases involving classical statistics and transition to degeneracy The latter two cases are of interest here because they are directly applicable to semiconductors

The present work in general involves measurements on specimens in which the concentration of charge carriers is sufficiently small that classical statistics may be used to obtain a good approximation The spin susceptibility of a free electron or hole gas can be readily calculated by a simple method in which the chemical approach is used The concentration of free electrons in a classical semiconductor without regard to spin is given by

$$n_e = \frac{2(2\pi mkT)^{3/2}}{h^3}\, e^{\zeta/kT} \tag{5}$$

The electrons of one spin orientation are in equilibrium with those of the other orientation and in

the absence of a magnetic field the concentrations are equal

$$(6)\quad \vec{n}_e(\vec{H} = 0) = \overleftarrow{n}_e(\vec{H} = 0) = \frac{(2\pi mkT)^{3/2}}{h^3} e^{\zeta/kT}$$

However in the presence of a magnetic field the energy of the parallel spin state is lowered by an amount βH while that of the antiparallel state is raised an equal amount Hence

$$(7)\quad n_e = \vec{n}_e(\vec{H}) + \overleftarrow{n}_e(\vec{H}) = \frac{(2\pi mkT)^{3/2}}{h^3} e^{\zeta/kT} (e^{\beta H/kT} + e^{-\beta H/kT}) = \frac{2(2\pi mkT)^{3/2}}{h^3} e^{\zeta/kT} \cosh \frac{\beta H}{kT}$$

where ζ is the Fermi level or free energy per electron irrespective of the spin in the magnetic field Since n_e may be taken as fixed, it is evi dent from Eqs 5 and 7 that

$$(8)\quad e^{\zeta/kT} \cosh \frac{\beta H}{kT} = e^{\zeta/kT}$$

By expanding the cosh term and discarding all terms above those involving H^2 it is seen that

$$(9)\quad \Delta\zeta = \zeta - \zeta = kT \ln \left[1 + \frac{1}{2}\left(\frac{\beta H}{kT}\right)^2\right]$$

At $T = 300°K$ and $H = 30\,000$ gauss $\Delta\zeta = 6\ 1 \times 10^{-7}$ ev With the use of equation 5 it is seen that the applicable range of ζ at $-100°C$ for carrier concentrations between 10^{14} and 10^{18} cm^{-3} is $0\ 10 > \zeta > 0\ 01$ ev Hence it is apparent that the value of ζ is not significantly changed by fields readily obtainable in the laboratory, and, as a consequence the zero field value of ζ may be used without loss in accuracy The total mag netic moment per unit volume from free carriers is given by the product of the Bohr magneton and the difference in concentration of the two spin states

$$(10)\quad M = \beta\left[\vec{n}_e(\vec{H}) - \overleftarrow{n}_e(\vec{H})\right] = \frac{\beta(2\pi mkT)^{3/2}}{h^3} e^{\zeta/kT} (e^{\beta H/kT} - e^{-\beta H/kT}) = \frac{2\beta(2\pi mkT)^{3/2}}{h^3} e^{\zeta/kT} \sinh \frac{\beta H}{kT}$$

Expanding the sinh term and discarding the higher order terms gives

$$(11)\quad M = \frac{2\beta^2 H}{kT} \frac{(2\pi mkT)^{3/2}}{h^3} e^{\zeta/kT} = n_e \frac{\beta^2 H}{kT}$$

The volume susceptibility as a result of spin only is

$$(12)\quad \kappa = \frac{M}{H} = \frac{n_e \beta^2}{kT}$$

In addition to the paramagnetism resulting from the spin of a free electron the diamagnetism as sociated with the orbital motion imparted to it by the magnetic field must be considered Treat ment of this problem by classical mechanics indi cates that there is no resultant diamagnetism that is the total moment of electrons reflected at the boundary of the container exactly cancels the moment of the electrons in the interior [17] How ever Landau[24] examined the problem from the standpoint of quantum mechanics and found that there is a diamagnetic contribution for completely free electrons which is exactly one third the spin paramagnetism Consequently the resultant sus ceptibility for a perfectly free classical electron gas is two thirds the value given by Eq 12 Stoner includes the Landau term in his final calculations More recent studies of the diamagnetism of free electrons have been made by Sondheimer and Wilson [44] Osborne,[31] and Steele[46] in order to check certain questionable points in Landau s work The results of these more thorough investigations confirm the early work in all important details

Conduction electrons and holes in solids are not entirely free and therefore the free electron treatment is only an approximation The first attempt to take crystalline field forces into consideration was made by Peierls[34] with application to metals In passing over from the completely free to the completely bound state the electron loses its paramagnetic character resulting from spin and the diamagnetic contribution becomes $(-e^2/6mc^2)\overline{r}^2$ where $\overline{r}^2$ is the mean square orbital radius It is to be noted that this is the same as the expression obtained for orbital diamagnetism by using classical considerations In solids where conduction particles are nearly free crystal forces may be taken into approximate account in using the free electron treatment by means of an effective mass m a quantity of the same order of magnitude as the electronic rest mass This method of approximation is better the more free the charge carrier and begins to break down as the carriers become more tightly bound This approach is very convenient in the case of germanium where it gives a reasonably good approximation

$$\chi = \chi_a + \frac{\beta^2}{3\rho kT}\left[6 - f_e^2 - f_h^2\right] \frac{2(2\pi mkT)^{3/2}}{h^3(f_e f_h)^{3/2}} e^{-E_g/2kT} \tag{17}$$

In a manner similar to that used by Busch and Mooser [9] the specific susceptibility of an impurity semiconductor may be written as the sum of the contributions of (1) the diamagnetic susceptibility of germanium atoms combined in the lattice χ_a (2) the paramagnetic susceptibility χ_I of the unionized impurities with an odd number of electrons

$$\chi_I = \frac{\beta^2}{\rho kT}(N_{D_i} - n_i) \tag{13}$$

(3) the paramagnetic susceptibility of the charge carriers as a result of spin χ_s

$$\chi_s = \frac{\beta^2}{\rho kT} n_i \tag{14}$$

and (4) the diamagnetic contribution from orbital motion of the charge carriers caused by the magnetic field

$$\chi_c = \frac{\beta^2}{3\rho kT} n_i f_i^2 \tag{15}$$

where ρ is the density of germanium N_D is the number of ionizable impurities and f and n are the freedom number ($f = m/n^*$) and the number of current carriers per cubic centimeter respectively In an n type semiconductor the subscript i refers to conduction electrons and in a p type to holes Thus

$$\chi = \chi_a + \chi_I + \chi_s + \chi_c = \chi_a + \frac{\beta^2}{3\rho kT}(3N_{D_i} - n_i f_i^2) \tag{16}$$

For a pure intrinsic semiconductor χ_I is zero and the number of holes equals the number of electrons By using the carrier product of Eq 2 χ becomes

The effect of fast neutron bombardment might be expected to alter the magnetic susceptibility of germanium in one or more of several ways The lattice disorders produced by fast neutron bombardment and cold work have been shown to have a similar effect on the plastic properties of some metals [3] The results of measurements by Bitter[6] and by Honda and Shimizu[20] indicate that the susceptibility of copper is sensitive to cold working in at least one case it changed from negative to positive and returned to negative after annealing However in copper there are no covalent bonds to be broken in the disordering process as there are in germanium

From Eqs 14 and 15 it is apparent that the contribution of the current carriers to the total susceptibility is paramagnetic if the freedom number is less than $\sqrt{3}$ zero if it is $\sqrt{3}$ and diamagnetic if it is greater than $\sqrt{3}$ A change in the number of carriers by bombardment would affect their contribution to the susceptibility accordingly If the carriers are trapped as unpaired electrons in s like orbits a paramagnetic contribution could be expected and if they are trapped as pairs with opposed spins only a very weak diamagnetic contribution would be found The results of this work have been carefully scrutinized in the light of these various possibilities

CHAPTER 2 INSTRUMENTATION

1 MAGNET AND CONTROLS

An Arthur D Little Inc Bitter type[7] of electromagnet was used When supplied by a 25-kw converter magnetic fields in excess of 25 kilogauss were obtainable across pole faces $5\frac{3}{4}$ in in diameter separated $1\frac{1}{4}$ inches Figure 1 shows a general view of the magnet and the other apparatus pertaining to the work Figure 2 is a close up of the south yoke with the north yoke backed away to expose the south pole of the magnet (the truncated cone) Extending over the pole face are the cryostat sample tube and the Dewar for maintaining the field control crystal at constant temperature Not shown in either figure are the 25-kw amplidyne converter power unit and the yoke coolant pump and heat exchanger The magnet is mounted on a sheet steel housing (to allow room for necessary plumbing) which in turn rests on critically loaded heavy duty vibration stripping

Control devices[35] permitted the reproduction and maintenance of magnetic fields in the range of 5 to 25 kilogauss with a precision of better than 0 05% The output of the power unit was adjustable and it stabilized to approximately 1% constancy The Hall voltage produced across a germanium crystal located in the pole gap provided direct field control by regulating an auxiliary current flowing in trimmer coils located in the magnet yokes The latter device although having limited field correcting range was operated in conjunction with the power unit controls and thus provided control over the entire range

In operation the voltage drops across various components of the control system were measured with a potentiometer and adjusted to values determined by the field desired The ultimate reference for reproducing given fields was therefore a standard cell Since the method does not require an exact knowledge of the value of the field but rather only the reproduction of previously selected fields an exact calibration of the field is not necessary

Figure 3 is a plot of H^2 vs z the radial distance from the axis of the magnet under five conditions of magnet excitation the arrow indicates the edge of the pole face A gap of $1\frac{1}{4}$ in was used throughout all this work These data were obtained to locate the region of maximum force (maximum gradient of H^2) for Faraday type measurements of magnetic susceptibility The measurement of the Gouy force on an 0 008 in dia platinum wire was used to determine H^2

The shape of the $H\ dH/dz$ field as determined for only one condition of magnet excitation is shown in Fig 4 This plot was obtained by the measurement of the Faraday force on a 5-mm germanium cube The two plots (Figs 3 and 4) were used to locate the region in the field wherein the germanium samples were to be suspended for the determination of the magnetic susceptibility

2 BALANCE CHAMBER AND ASSOCIATED GAS VACUUM EQUIPMENT

In essence the balance chamber consisted of an iron bell jar system mounted on the south yoke of the magnet as shown in Figs 1 and 2 for Fig 2 the bell jar was removed to expose the balance The cryostat sample tube hangs from beneath the bell jar plate into the pole face region Although the magnet is of a closed loop design stray fields are generated outside the loop when it is operated at high fields The bell jar (hereafter referred to as the tank) and the bell jar plate (henceforth the plate) were fabricated from mild steel and then annealed to provide magnetic shielding for the balance However only partial magnetic shielding was obtained The plate supports were made of angle iron with sections replaced with brass bar stock to eliminate easy magnetic paths from the magnet to the bell jar system The tank plate and other iron or steel parts in the region of the balance and sample tube were cadmium plated to reduce the likelihood of contaminating samples with ferromagnetic surface impurities

The plate was 17 in in diameter and 1 in thick Holes through this plate accommodated multiple Kovar to-glass seals for balance chamber thermocouples and electrical lead throughs to the balance The balance beam rest mechanism was actuated by a rod that extended through the plate and was sealed with a brass bellows Extension or compression of the bellows by turning an outside cam imparted vertical motion to the rod inside the vacuum chamber In the unlocked position the rod made no contact with the balance or its intermediate mass plate

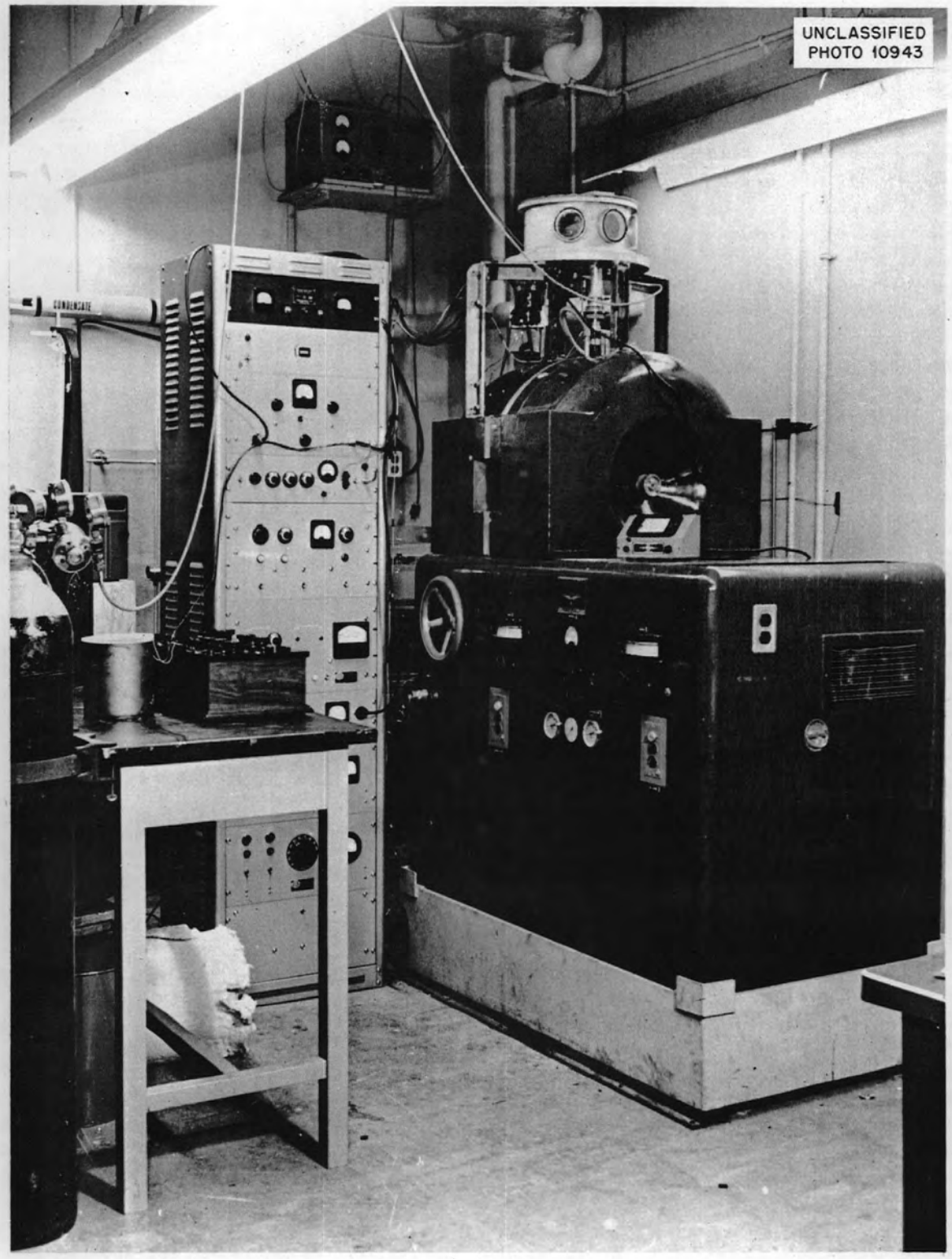

Fig. 1. Magnetic Susceptibility Laboratory

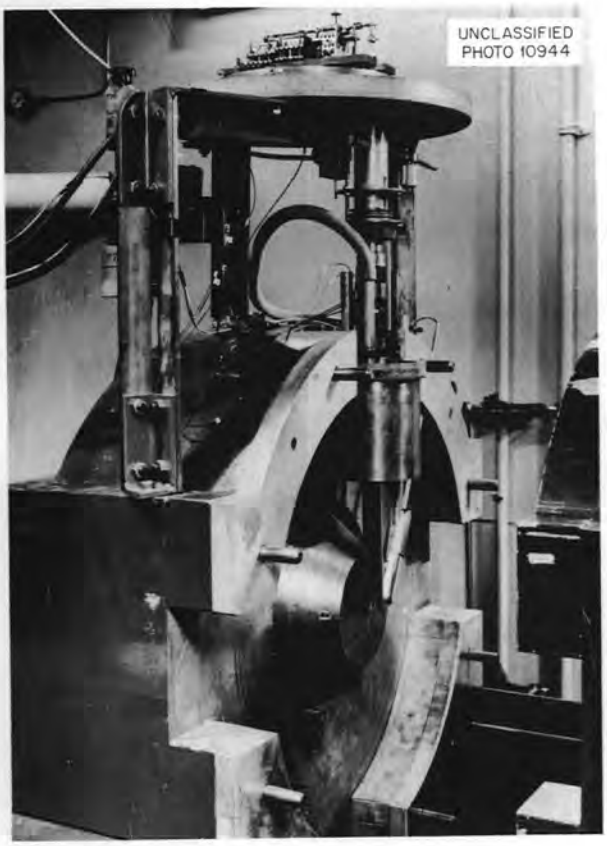

Fig. 2. South Yoke and Pole of the Magnet Showing Portion of Cryostat and Control Crystal Dewar.

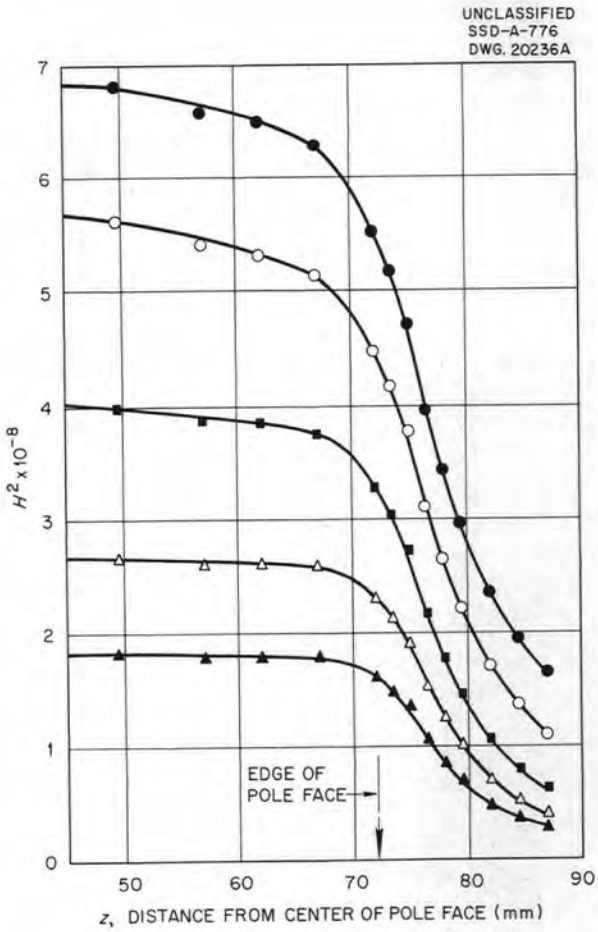

Fig. 3. H^2 vs. z.

The tank was fabricated from a 6-in. length of $12\frac{3}{4}$-in.-dia seamless steel tubing with a $\frac{3}{16}$-in. wall. Flanges to accommodate O-ring gaskets were brazed to each end, and three 3-in. view ports of $\frac{1}{4}$-in. pyrex glass were provided. The tank lid was simply a 14-in.-dia steel disk, $\frac{3}{16}$-in. thick, provided with a frame into which was waxed a pyrex window, $2\frac{1}{2}$ by $7\frac{1}{2}$ inches. This window was located directly over the balance and sample-tube opening. The lid was bolted to the tank and the tank was bolted to the plate; O-ring gaskets provided the vacuum seals.

The cryostat-sample tube was attached to a $1\frac{1}{2}$-in.-dia steel pipe which extended through the plate and was heliarc welded to it at a position vertically over the pole gap. This pipe may be seen in Figs. 1 and 2. The O-ring flange to which the cryostat was attached was joined to this pipe through a brass bellows and three spacer bolts which permitted the alignment of the cryostat. A Hastings thermocouple vacuum gage and the gas inlet valve were also located on this pipe.

Pumping equipment for the balance-sample chamber consisted of a Distillation Products, Inc., VMF-10, air-cooled, oil diffusion pump and a Welch, Duo-Seal 1405, mechanical pump. Since the highest vacuum sought was between 1 and 10 μ Hg, cold traps were unnecessary. The purpose of the diffusion pump was to provide the pumping speed desired below 100 μ during outgassing operations. The pumps were connected to the system through the plate.

Except during calibration with oxygen at room temperature, all measurements were conducted in an atmosphere of helium at approximately 100 μ Hg. At this pressure, helium provides good thermal transfer between sample and sample-tube wall without the danger of objectionable convection currents. Insofar as this work is concerned, the

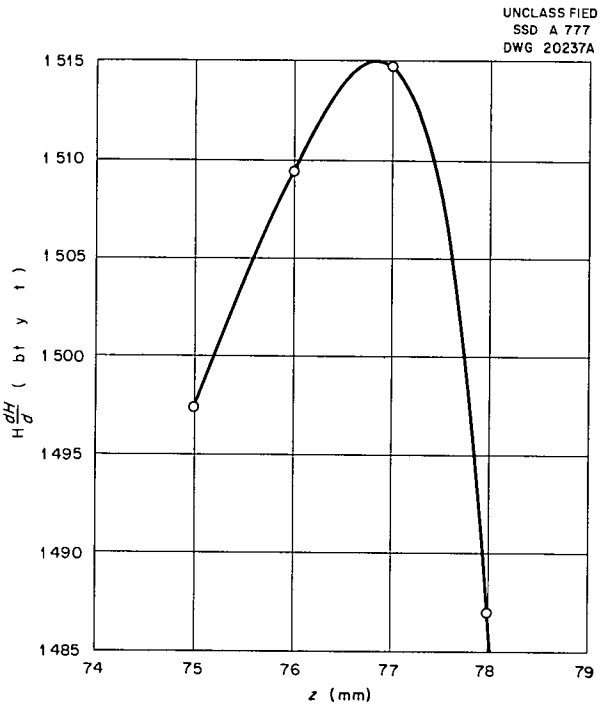

Fig 4 $H\,dH/dz$ **(relative) vs** z

heat transfer characteristics of helium do not vary appreciably with pressure at pressures above 75 μ Hg and buoyancy effects are negligible An uncalibrated thermocouple gage was sufficient for pressure indications Since it was not feasible to completely outgas the system a dynamic pressure of 100 μ was employed The valve to the pumping system was adjusted so that when the valve to the helium system was cracked and a minute helium leak was maintained a pressure of 100 μ as indicated by the gage was obtained

All magnetic measurements were made relative to oxygen gas at a pressure of 760 mm Hg at room temperature Oxygen pressures were adjusted to that value as indicated by a manometer previously calibrated against a Fortin type barometer Since accuracy to only 0 5 mm was required the calibration at atmospheric pressures (735 to 745 mm) was extrapolated to 760 mm

The gas system is shown schematically in Fig 5 Tank oxygen was passed through a palladium catalyst to burn out traces of hydrogen and then through a solid CO_2 acetone trap to remove water before entering the balance sample system According to the manufacturer s claims the product should be 99 7% pure with nitrogen being the only impurity other than hydrogen Analyses for total oxygen indicated 99^{+}% after passage through this train Because the magnetic susceptibility of oxygen is higher by a factor of 200 or more than that of any gas other than nitric oxide only the total oxygen determination was needed for these calibrations Before entering the system the U S Bureau of Mines Grade A helium to be used was passed through an activated coconut charcoal trap in a liquid nitrogen bath to remove any oxygen present Between runs this trap was warmed to room temperature and the absorbed gases were pumped off

3 CRYOSTAT

The cryostat may be described as a continuously pumped metal Dewar equipped so that the temperature of the lower part of the inner tube can be easily maintained at temperatures between 90 and 300°K By using an exchange gas helium in this case the temperature of a sample suspended therein could be controlled Figure 2 shows the cryostat suspended in place below the plate

Figure 6 is a schematic representation of the device F indicates the inner or sample tube which down to a point about opposite J is made of copper nickel tubing with a wall thickness of 0 010 inch Below this point it is a copper tube $^5/_8$ in in outside diameter and 0 035 in in wall thickness The 9$^1/_2$ in long copper nickel section serves to isolate thermally the lower section A hollow donut shaped refrigerant vessel G is suspended in the continuously evacuated space between the sample tube and the outer jacket H At J the refrigerant vessel is thermally connected to the copper sample tube by a 0 002 in thick flat copper foil ring soldered across the annular gap separating the two parts Immediately below this copper foil an electrical resistance heater K is clamped to the copper sample tube Three copper constantan thermocouples, No 30 B S gage, are soldered to the outside of the copper sample tube one near the bottom (couple 2) one opposite the sample (couple 3), and one just below the heater (couple 4) The temperature of the sample tube is determined by the temperature of the refrigerant vessel the thermal resistance of the copper foil and the heat influx from room temperature radiation and the heater winding The Dewar vacuum is maintained by continuous pumping with an air

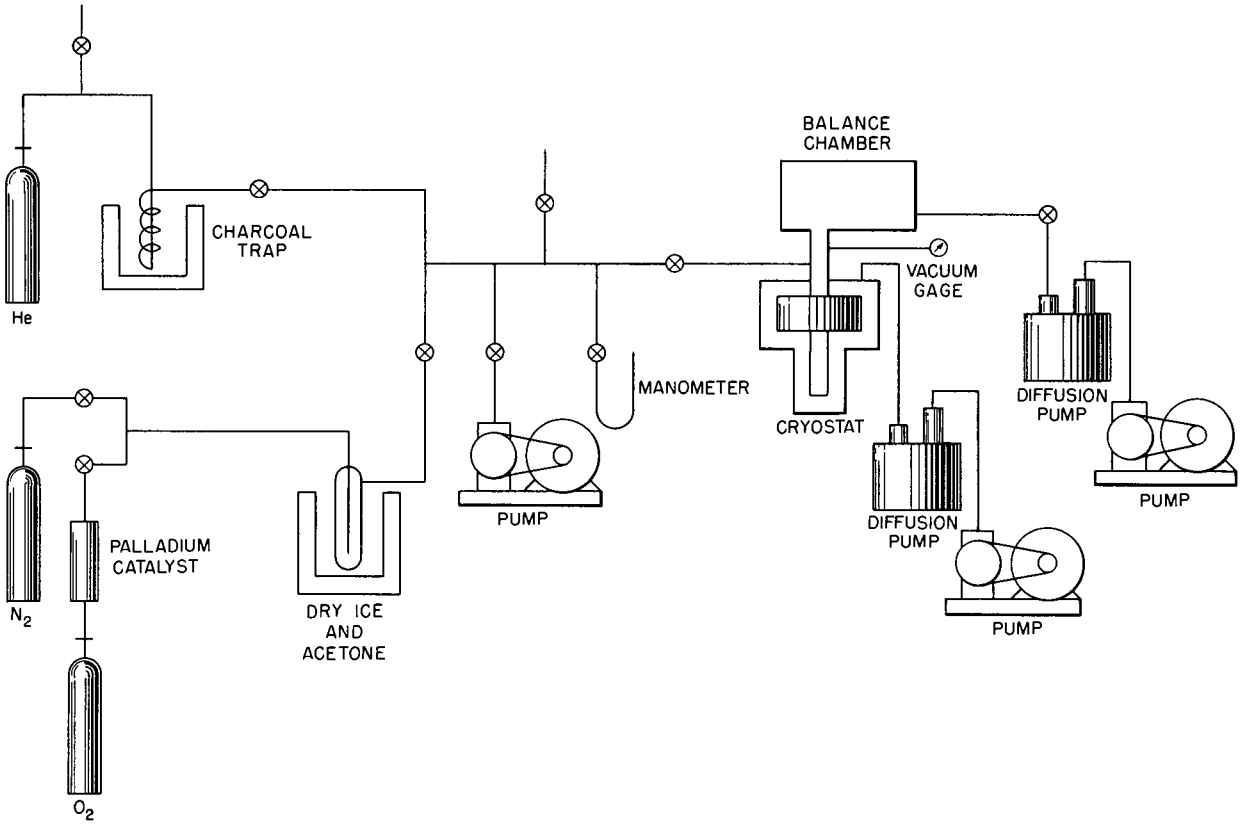

Fig 5 Schematic Diagram of Vacuum and Helium Oxygen Systems

cooled DPI VMF 10 oil diffusion pump and a Welch Duo Seal 1405, forepump

Heat transfer across the Dewar vacuum and room temperature radiation streaming down the sample tube maintain it at 11°C above the temperature of the refrigerant vessel (–196°C) when the latter contains boiling liquid nitrogen at atmospheric pressure Ten watts of electrical energy through the heater will raise the sample tube temperature 125°C above the refrigerant vessel temperature By continuous pumping of the refrigerant vessel when filled with liquid nitrogen sample tube temperatures as low as 65°K (–208°C) have been obtained At liquid nitrogen temperature there appears to be a temperature difference down the copper sample tube of approximately 1°C although the difference between couples 2 and 3 is less than 0 1°C Experiment indicated that the temperature of a dummy sample agreed to within ±0 1°C with the temperature indicated by couple 3 in the temperature range from 89°K to room temperature when the pressure of the helium exchange gas was above 75 μ Hg as indicated by the uncalibrated thermocouple gage

The thermocouple and heater leads were clamped to the sample tube and refrigerant vessel walls and brought out through hollow multiple Kovar glass seals in the top of the cryostat wax was used to provide the vacuum seal between the wires and Kovar tube walls Liquid nitrogen was blown into the refrigerant vessel down one of the vertical pipes visible in Fig 2

4 THE BALANCE AND ITS ASSOCIATED CIRCUITRY

The balance constructed for this research uses an electromechanical transducer as the balance point indicator an electromagnetic load measuring device and torsion fibers for suspensions instead of knife edges The assembled balance is shown

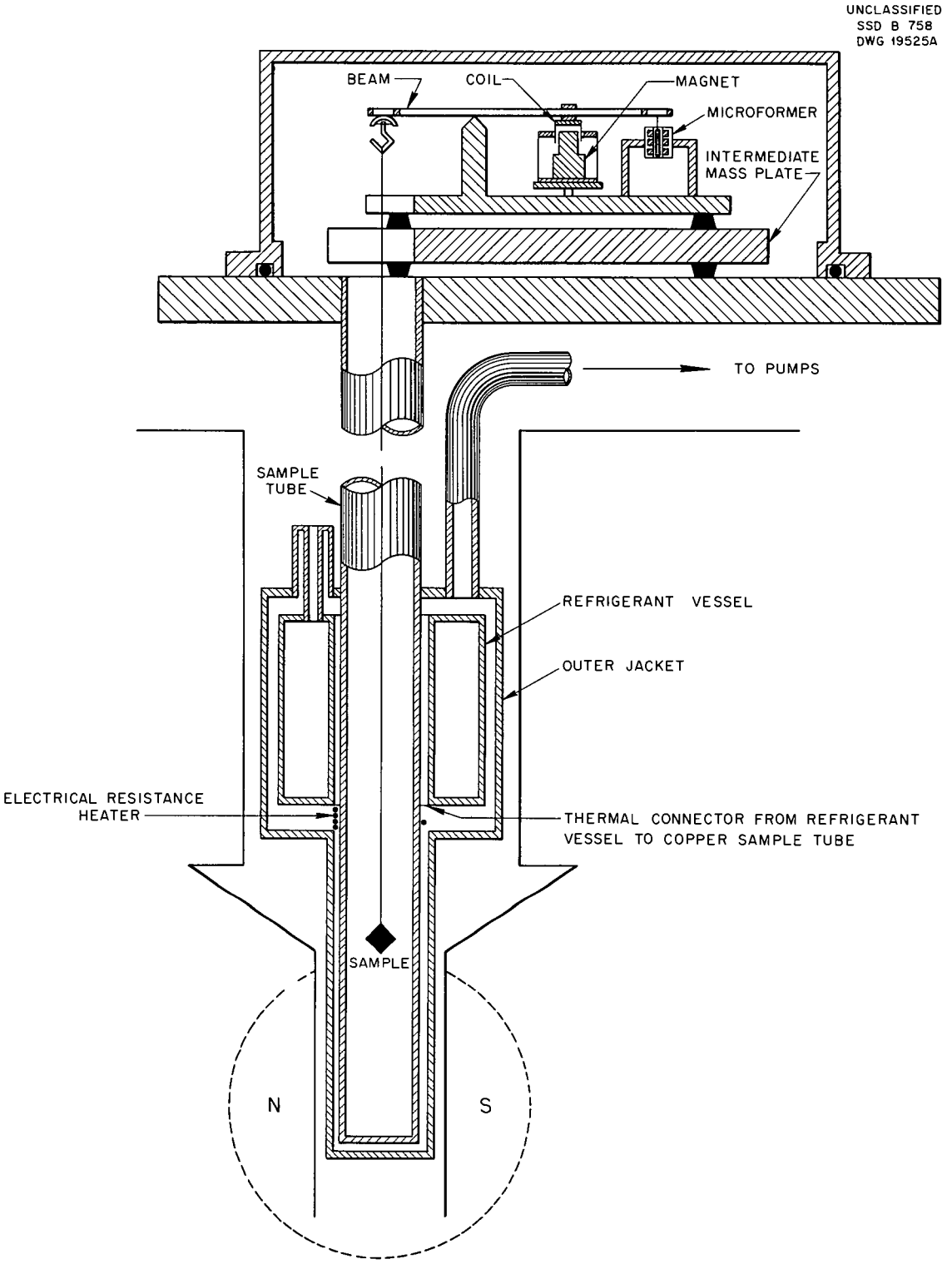

Fig 6 Magnetic Susceptibility Equipment

in Fig. 7; it is a modification of the balance originally reported by Hutchison and Reekie[21] and later improved by McGuire and Lane.[26] The sensitivity of the instrument has been increased by a factor of approximately 500, the latter authors having reported $\frac{1}{20}$ of a dyne as the limit of detectability. It is used as a differential balance in the present application.

The beam, A, in schematic Fig. 6, is a gold-plated, hardened-beryllium-copper, $\frac{1}{8}$-in. rod supported by a torsion ribbon of Elgiloy,[53] 0.025 by 0.0036 by 1.25 in. in total torsion length.* Samples are suspended from a universal joint consisting of a system of smaller torsion fibers and hooks 2 in. from the main axis of torsion. Restoring forces are applied to the beam from a 5-in. loud speaker by means of the voice coil and the permanent magnet assembly; the coil, B, is attached to the beam, and the magnet, C, is attached to the base. The beam position is indicated by the output signal from an electromechanical transducer, D, a linear differential transformer, which is hereafter referred to as the microformer. These elements of the balance will be treated in more detail below. The beam, its supporting yoke and beam rest mechanism, and the speaker magnet and microformer stages are mounted on a $\frac{1}{4}$-in. brass plate, the total weight being 4 pounds. This assembly is mounted on an intermediate mass plate, E; four, 1-lb-capacity, Lord, rubber, shock mounts are used. The brass intermediate mass plate is, in turn, supported off the plate by four, 4-lb-capacity, Lord, shock mounts, the total weight of the assembly being 16 pounds. These two critically loaded vibrational systems in combination with the shock mounting of the massive magnet serve to isolate the balance from all environmental vibrations except those of extraordinary amplitude.

The major contribution to the increased sensitivity of the balance over its precursors is the use

*The Elgiloy was furnished by the Elgin National Watch Co.

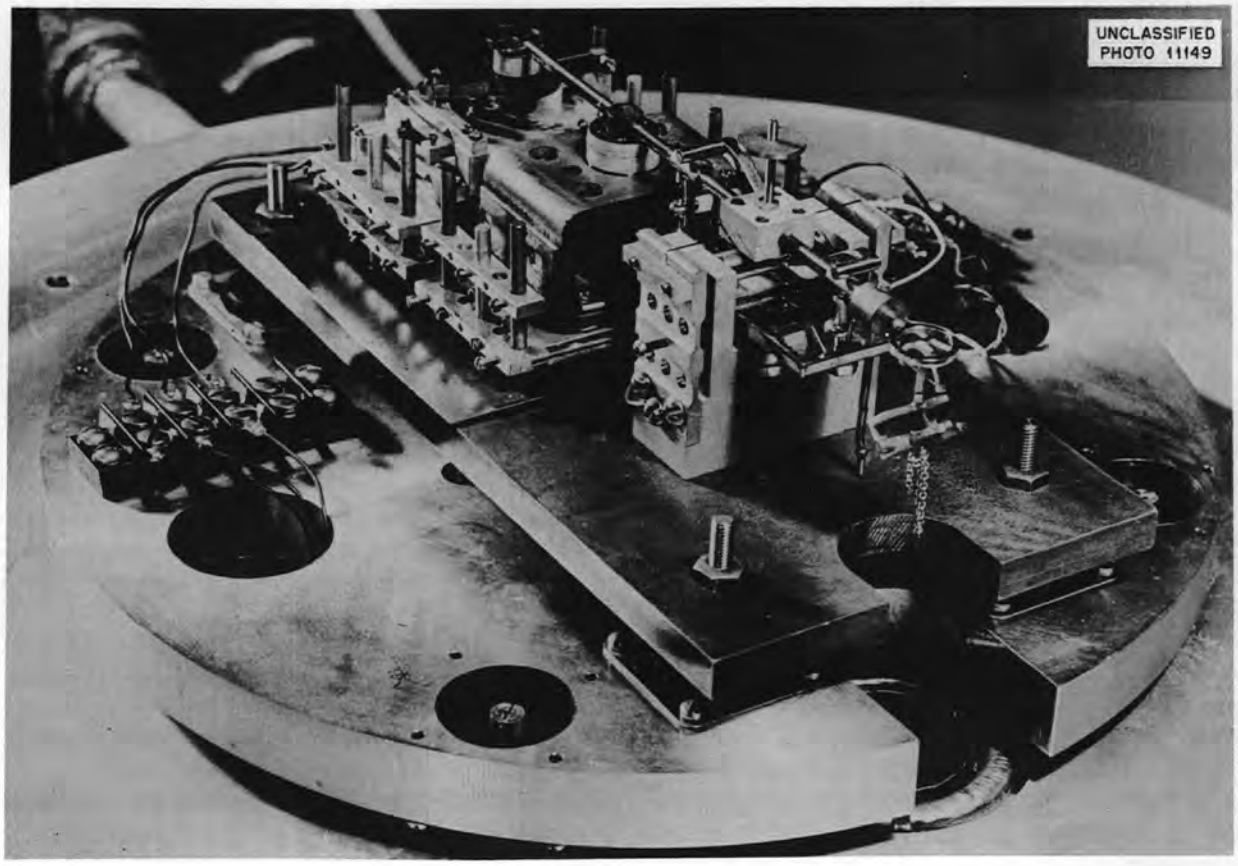

Fig. 7. Electrodynamic Torsion Microbalance.

of the microformer to indicate the balance position of the beam This device is visible at the far end of the beam in Fig 7 and is shown schematically as D in Fig 6 The microformer is a transformer with a movable iron core and twin secondary coils which are mounted axially and separated by the primary coil The secondary coils are connected so as to electrically oppose each other and when the iron core takes a position that causes equal induction in each there is no resultant signal in the secondary circuit A slight change in the core position will cause unequal induction and a resultant signal will be produced the phase of which is dependent upon which coil is receiving the greatest induction With proper circuitry the device is capable of signaling movements of the core of the order of microinches

In the present application the iron core with mass of the order of 1 g is suspended from the beam down the axis of the microformer The latter is mounted on a system of adjustable levers off the base of the balance The position of null signal is used as the balance point of the beam The electronic circuit used is shown in Fig 8 the microformer being designated by E MT Condensers C_1 and C_2 are chosen to correct any lack of electrical symmetry in the two secondary coils The sensitivity of the device is dependent upon the outputs of the secondaries being exactly in phase with each other The meter M in the phase detection section of the circuit is a 25 0 25 microammeter which indicates the beam position the balance point being 0 Switch S_2 is a gain switch which operates in factors of 10 In the high gain position a 1 μg change in balance load causes a meter deflection of approximately 5 microamperes

The force of interaction between a current carrying conductor and an independent magnetic field is used to counterbalance and measure changes in loads on the balance If it is assumed that the independent magnetic field is uniform or that the conductor maintains a fixed position this force is proportional to the product of the current times the field The coil from a 5 in speaker (B in Fig 6) is attached to the balance beam while the permanent magnet C and its yoke are mounted on the balance base The current flowing in the speaker coil is adjusted until the beam has returned to the null position as indicated by the microformer At balance the coil is always in the same position in the field and as a consequence the force of interaction is proportional only to the current This assembly is shielded from stray magnetic fields

Figure 9 is a schematic circuit diagram of the direct current supply to the balance arm coil The magnitude of the current is determined by measuring, on a potentiometer the voltage drop across a standard 100 ohm resistor in series with the supply A reversing switch permits the measurement of both positive and negative changes in the balance load The main beam suspension provides current leads to the speaker coil This ribbon is not continuous being broken in the middle and electrically insulated from the base and the beam One leg of the circuit is connected both to the ground and to the beam however to avoid electrostatic disturbances to the balance

In order to determine the balance characteristics calibrations were conducted by using 1 and 10 mg class M riders The balance response was found to be linear within the error of the measurement and the calibration was found to hold for a period of ten days at constant load to within 0 1% when determined by using the 10 mg weight The current response was found to be 0 2518 ± 0 0002 ma per 10 mg

The main suspension ribbon was fabricated of Elgiloy Its proportional limit is approximately two and one half times that of material previously used and thus a thinner ribbon could be used without sacrificing strength As the torsional restoring force of a twisted ribbon of rectangular cross section is a power function of its thickness small reductions in thickness are of importance in the present application Ideally a ribbon material with no resistance to torsion would be desired In this respect the principles given in U S Patent No 2 238 380[1] were incorporated in the design of all the suspension fibers The ribbon material was twisted into a helical form and heat treated so that it would retain this shape and to increase its hardness Upon incorporation in the balance the ribbon was clamped in an untwisted stressed condition so that when the beam was rotated through small angles the stress in one of the sections of the support was increased and the stress in the other was reduced According to the patent the choice of the proper angle of pretwist would result in a net effect of no resistance to torsion for small deflections around the equilibrium position No extensive tests were carried out to determine the effect of this feature on the balance sensitivity

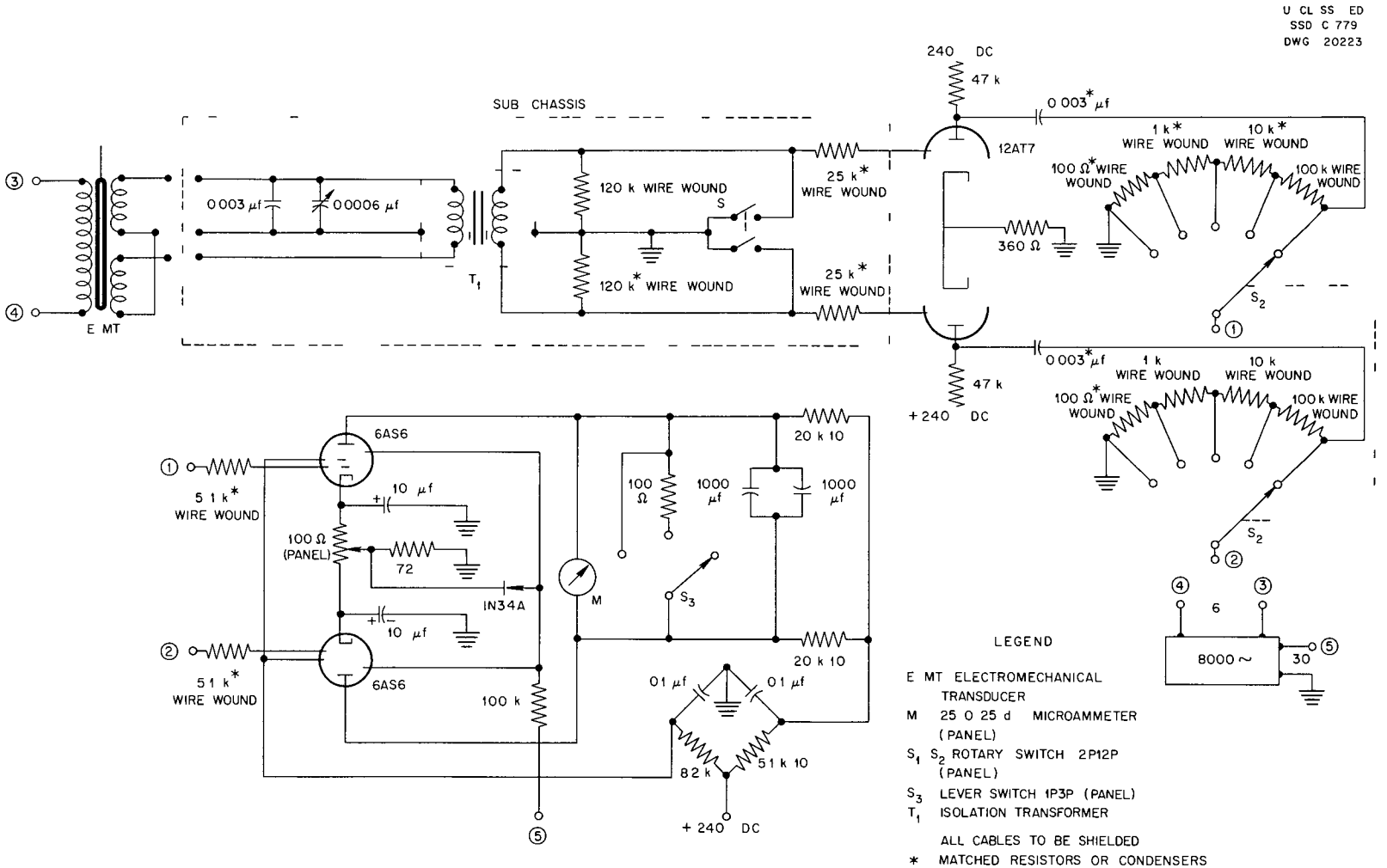

Fig 8 Amplifier Phase-Sensitive Detector Circuit for Microbalance

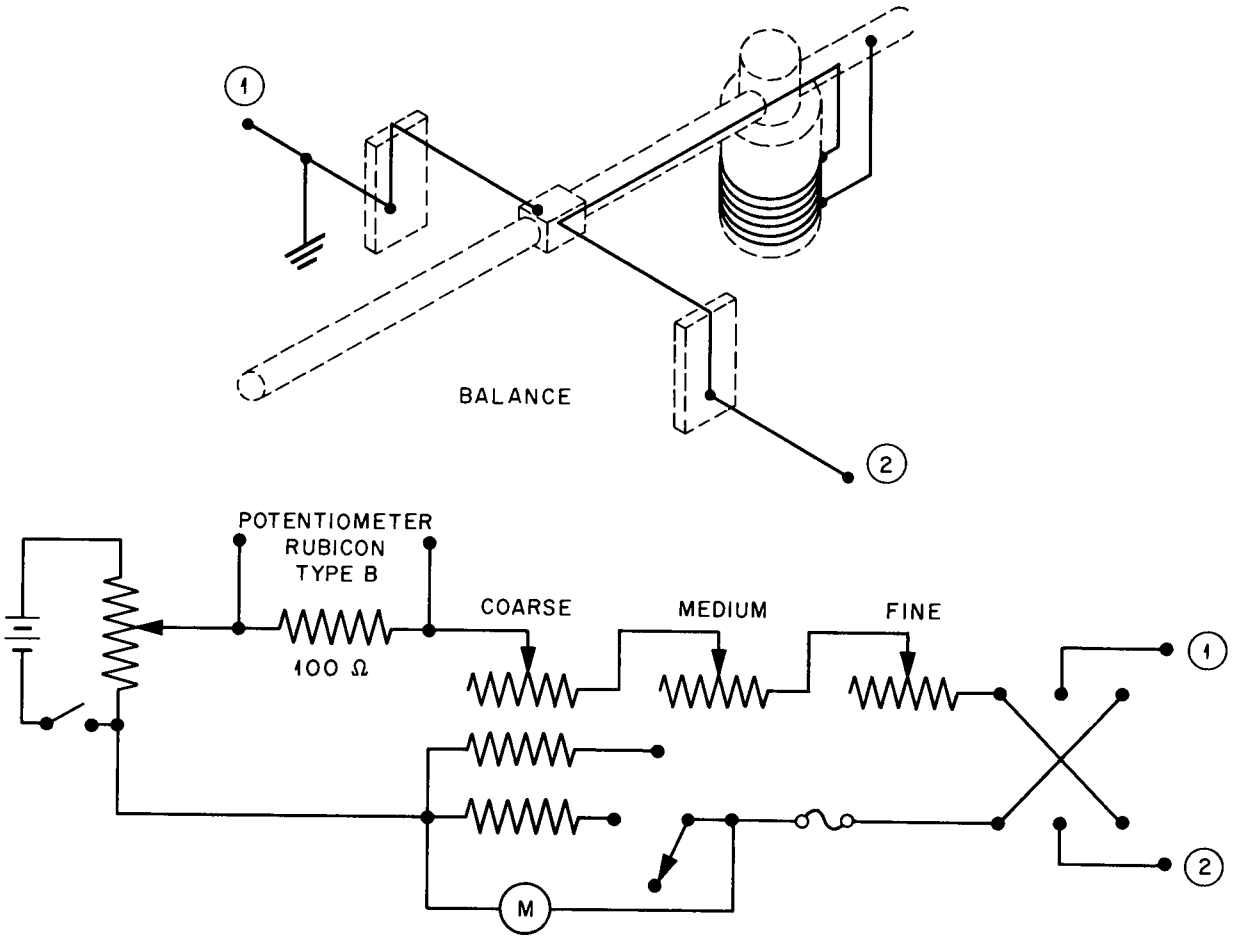

Fig 9 Direct Current Supply for Microbalance

The yoke on which the beam was mounted was machined from type M Lavite an inorganic material whose coefficient of linear expansion closely approximates that of the Elgiloy A beam rest mechanism visible in Fig 7 was incorporated in the balance to limit beam rotations and to protect the suspension fiber when samples were changed This beam rest mechanism could be operated from outside the vacuum system

Samples were suspended from a universal joint consisting of crossed torsion fibers so that the load to the beam was effectively applied at a point The sample lever arm was therefore of fixed length Samples were hung from this system on 0 001 in dia molybdenum wire The center of gravity of the balance arm was adjustable by using a weight on a screw at the suspension head

Figure 10 is a plot of the reciprocal of magnetic susceptibility in arbitrary units of a ball of platinum wire (approximately 100 mg) vs absolute temperature measured by using the equipment described above Lack of adherence to a straight line would indicate failure of one or more units of the equipment to operate properly The solid circles represent preliminary order of magnitude measurements while the open circles represent data gathered by using the techniques developed for the work on germanium

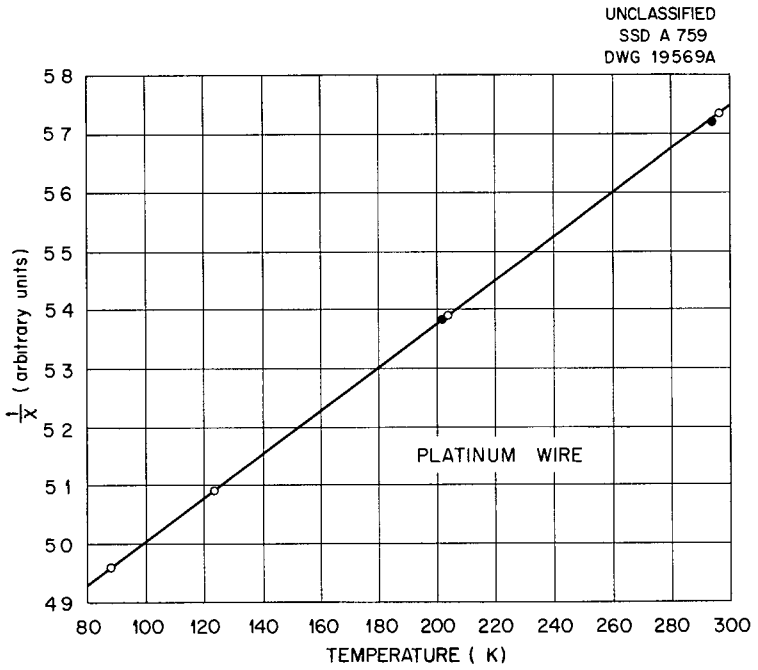

Fig 10 $1/\chi$ vs T of Platinum Wire

CHAPTER 3 EXPERIMENTAL PROCEDURES

1 FORMULAS AND EQUATIONS[2 41]

The force exerted on a body suspended in an inhomogeneous magnetic field (the Faraday method) is given by

$$(1) \qquad F_0 = \frac{m}{\rho}(\kappa - \kappa_0) H \frac{dH}{dz}$$

where F is the force in the z direction measured in dynes m and ρ are the mass in grams and the density of the body κ and κ_0 are the volume susceptibilities of the body and its surrounding medium, respectively H is the field in gauss and dH/dz is the field gradient in the z direction When the body is suspended in a vacuum κ_0 equals zero and the expression reduces to

$$(2) \qquad F_v = \frac{m}{\rho} \kappa H \frac{dH}{dz} = m\chi H \frac{dH}{dz}$$

where χ is the specific susceptibility Subtracting Eq 2 from Eq 1 and solving for $H\ dH/dz$ (the specific force) gives

$$(3) \quad H\frac{dH}{dz} = -\frac{\rho}{m}\frac{F_0 - F_v}{\kappa_0} = -\frac{F_0 - F_v}{V\kappa_0}$$

The effective value of $H\ dH/dz$ for a given volume in the field is a function of the setting of the field controls of the magnet and is essentially independent of the properties of the material (for other than ferromagnetic materials) occupying the volume Thus for each setting of the magnet controls $H\ dH/dz$ is obtained by measuring the forces exerted on the sample when suspended in a vacuum and when suspended in another medium of known susceptibility the quantities used in this evaluation are designated by an asterisk in the following equation for χ which was obtained from Eqs 2 and 3

$$(4) \qquad \chi = -\frac{F_v}{F_0^* - F_v^*}\frac{\kappa_0^*}{\rho^*}$$

Therefore after calibration under specified conditions that is those conditions under which κ_0

and ρ are known the susceptibility of the sample may be determined at any temperature by measuring the force exerted upon it when it is suspended in a low vacuum Since the actual value of $H\ dH/dz$ for the volume in space occupied by the sample is measured the geometrical shape of the sample is unimportant provided the sample is magnetically isotropic the position of the sample in the field need not be determined precisely and the suspension length is not critical

The force exerted on the sample was determined by measuring its apparent change in weight when the magnet was energized In the description of the balance sec 4 of chap 2 it was pointed out that load counterbalancing forces were applied to the beam by a measured direct current I flowing in a speaker coil–magnet assembly and that the force applied was proportional to this current Since the ratio of forces applied in this manner is used in the determination of χ the proportionality constant cancels and the ratio of currents may be used Thus by this method tedious calibrations of the balance and the possibility of the calibration changing with load (the samples were not all of the same mass the range being from 0 6 to 1 2 g) were avoided The essential requirement was that the balance maintain its response characteristics throughout a given series of measurements (approximately 32 hr) Equation 4 in its particular application to this research takes the form

$$\chi = \frac{I_v}{I_0^* - I_v^*} \frac{\kappa_0^*}{\rho^*} \tag{5}$$

which for a given sample hanging in the field and a given setting of the magnet controls reduces to

$$\chi = CI_v \tag{6}$$

Since the saturation magnetizations of ferromagnetic materials are orders of magnitude larger than the magnetic moments induced in para and diamagnetics by fields obtainable in the laboratory traces of impurities that exhibit ferromagnetic properties can alter the apparent susceptibility of the sample appreciably In order to include ferromagnetic materials Eq 2 takes the form[2]

$$F = m\chi H \frac{dH}{dz} + m_I \sigma_s \frac{dH}{dz} = m\chi\ H \frac{dH}{dz} \tag{7}$$

for $m_I \ll m$

where m_I and σ_s are the mass and specific saturation magnetization respectively of the ferromagnetic impurity and χ and χ are the apparent and true susceptibilities respectively of the specimen Dividing Eq 7 by $mH\ dH/dz$ gives

$$\chi + \frac{m_I \sigma_s}{m} \frac{1}{H} = \chi \tag{8}$$

and it is found that by making several measurements of χ at different fields and plotting the apparent susceptibilities against the reciprocal of the field the intercept at infinite field ($1/H = 0$) is the true susceptibility of the body independent of ferromagnetic impurities The slope of the plot is an indication of the degree of purity of the specimen From Eq 8 it is apparent that one part of ferromagnetic iron (σ_s = 200 ergs/gauss) in 10^7 parts would alter the value of an apparent susceptibility of 10^{-7} by approximately 1% if it were measured by using a field of 20 kilogauss

2 METHODS OF MEASUREMENT

The specimens used for this work were prepared by the Physics Department of Purdue University Lafayette Indiana Single crystal ingots were grown by slowly withdrawing a seed crystal from the melt (the Kryopolus method) Samples in the form of ½ cm cubes and plates cut from adjacent portions of these ingots were provided It was assumed that the plates were representative of the companion cubes and they were used for all conductivity and Hall coefficient measurements Upon receipt the cubes were cleaned mechanically by using fine metallurgical polishing paper (0/4) and they were etched in a bath composed of 40% hydrofluoric acid 20% nitric acid 15% glacial acetic acid and 25% water After washing drying and weighing the samples were annealed in a vacuum at 450°C for 60 hr followed by programmed cooling to room temperature

A suspension which consisted of a length of 0 001 in dia molybdenum wire was tied to each specimen in such a manner that when the specimens were suspended from the balance one of the planes containing a set of the parallel diagonals of opposite faces was perpendicular to the field All the suspensions were approximately equal in length (±1 mm) Since the combined Gouy and Faraday force on this suspension was less than 0 01% of the Faraday force on the sample it was

unnecessary to apply suspension corrections to the measured forces

Immediately prior to placement in the equipment the specimen and its suspension were washed with hot 6*N* hydrochloric acid hot distilled water and c p acetone Subsequent measurements on all specimens indicated that the cleaning procedure was sufficient to remove all detectable ferromagnetic impurities Following this treatment the sample was transferred into the equipment with neither it nor the lower part of its suspension being touched After suspending a sample from the sample hook on the balance the position of a movable counterweight on the balance arm was adjusted until a current of 15 μa or less in the speaker coil–magnet assembly brought the beam to balance The bell jar was then closed and the system was pumped down overnight

The relative Faraday forces acting on the sample when it was suspended in a low vacuum and when it was suspended in oxygen were measured at room temperature for five settings of the field controls The low vacuum consisted of a helium atmosphere maintained at a dynamic pressure of approximately 100 μ Hg The oxygen pressures were maintained at 760 0 ± 0 2 mm Hg as indicated by a calibrated mercury manometer During this series of measurements care was taken to conduct the vacuum and oxygen measurements at a given field control setting and at the same temperature ±0 1°C From these data the room temperature susceptibility was calculated by using Eq 5 and by taking the volume susceptibility of oxygen[41] as $\kappa_0 = 0\ 1434 \times 10^{-6}$ at 20°C and 760 mm pressure The volume susceptibility of oxygen at temperatures other than 20°C was calculated from this value by assuming a $1/T^2$ relationship [2] Since there was no trend as a function of field that was indicative of a ferromagnetic impurity the room temperature susceptibility of the sample was taken to be the weighted average of the five values obtained

The measurements of the susceptibility of a given sample of germanium as a function of temperature were all made at the same setting of the magnet field controls The proportionality constant C of Eq 6 was calculated for this setting by using the room temperature susceptibility and the I_v obtained in the manner mentioned above This value of the proportionality constant was then used in conjunction with the I_v s measured in a helium atmosphere to calculate the susceptibilities at other temperatures Temperatures below room temperature were obtained by introducing liquid nitrogen into the cryostat refrigerant vessel and then adjusting the input into the electrical heater on the sample tube until temperature stability at the desired temperature was obtained Temperatures below 88°K were obtained by pumping on the liquid nitrogen filled refrigerant vessel until the system reached thermal equilibrium After the overnight pump out approximately 16 hr was required to make the necessary measurements for the calculation and construction of each susceptibility vs temperature curve

Upon completion of a temperature run the sample with its molybdenum suspension was removed from the equipment and stored in a pyrex tube Samples to be irradiated were carefully rolled in aluminum foil along with the suspension wire packed in an aluminum tube and irradiated in a water cooled hole in the ORNL graphite reactor The cubes were irradiated singly and the electrical resistance of a companion Hall crystal that was located adjacent to the aluminum tube was continuously recorded throughout the irradiation The electrical resistance and the Hall coefficients of these companion crystals were measured as a function of temperature before and after irradiation by J W Cleland assisted by E Schwartz After irradiation the susceptibility cubes were stored at room temperature for 48 hr to permit decay of the induced radioactivity They were then removed from the aluminum tubing and foil with care being taken to preserve the wire suspension washed with hot 6*N* hydrochloric acid hot distilled water and c p acetone and remounted in the equipment The measurements of χ as a function of field at room temperature and as a function of temperature were then repeated

CHAPTER 4 EXPERIMENTAL DATA

1 SAMPLE CALCULATION

A representative set of data obtained for a cube of germanium (Sb 5A I) is given in Table 1 The atmospheres in which the sample was suspended while the measurements were made are listed in column 1 and the pressures of these atmospheres are given in column 2 In column 3 are the temperatures of the cryostat sample tube at a point adjacent to the sample As pointed out earlier these temperatures have been found to correspond to the sample temperatures ±0 1°C The interpolated values of the current necessary to bring the balance to null with the magnet off and the sample in place are listed in column 4 These values were obtained by noting the time at which this current was measured before the magnet had been turned on and after the magnet had been turned off and interpolating for the value at the time at which the magnet on current was measured The currents necessary to bring the balance to null when the magnet was in operation are given in column 5 The algebraic differences between columns 4 and 5 as listed in column 6 represent the incremental balance currents necessary to counterbalance the Faraday forces exerted on the sample by the field The average values for given sets of data are listed in column 7 The negativity of the values listed in columns 6 and 7 indicates that the force exerted on the sample was in such a direction as to reduce the load on the balance the negative value is a general indication of a diamagnetic substance

The currents listed in the last column are of interest in the calculation of the susceptibilities and the determination of the constant C in Eq 6 of Chapter 3 The first and second figures in this column are I_0^* and I_v^* respectively and as such are useful in determining the value of the susceptibility of the sample at room temperature and in calibrating the equipment for the determination of the susceptibility at other temperatures The value of the volume susceptibility of oxygen at 296 3°K may be calculated from the 293 2°K

TABLE 1 DATA FOR GERMANIUM*

SAMPLE ATMOSPHERE	PRESSURE	TEMPERATURE OF SAMPLE TUBE (°K)	BALANCE CURRENT (ma × 10)			
			Magnet Off	Magnet On	Difference	Average
O_2	760 mm	296 3	−1 7624	+0 4282	−2 1906	
			−1 7623	+0 4292	−2 1915	
			−1 7619	+0 4297	−2 1916	
			−1 7612	+0 4303	−2 1915	−2 1914
He	100 μ	296 3	−1 6842	+0 0689	−1 7531	
			−1 6855	+0 0674	−1 7529	
			−1 6860	+0 0665	−1 7525	
			−1 6865	+0 0662	−1 7527	−1 7528
He	100 μ	101	−1 7884	+0 0340	−1 8224	
			−1 7887	+0 0343	−1 8230	
			−1 7888	+0 0343	−1 8231	−1 8228

Sample Sb 5A I weight 1 098 g field t ample 18 kiloga ss
Interpolated value

value[41] by assuming proportionality to $1/T^2$ for constant pressure

$$\kappa_0^* = \kappa_{0_2} \left(\frac{293\ 2}{296\ 3}\right)^2$$

$$= (0\ 1434 \times 10^{-6})\ (0\ 9791)$$

$$= 0\ 1404 \pm 0\ 0004 \times 10^{-6} \text{ cgs units}$$

Since the coefficient of expansion of germanium[49] is small ($a = 5\ 92 \times 10^{-6}$) the density of germanium[49] at 25°C may be used for the density at the calibration temperature

$$\rho^* = 5\ 3234 \pm 0\ 0025 \text{ g/cm}^3$$

By substituting into Eq 5 of Chapter 3 it is found that the susceptibility at 296 3°K is

$$\chi = -\frac{I_v}{I_0^* - I_v^*}\frac{\kappa_0^*}{\rho^*}$$

$$= -\frac{0\ 17528}{-0\ 21914 - 0\ 17528}\ \frac{0\ 1404 \times 10^{-6}}{5\ 3234}$$

$$= -1\ 054 \times 10^{-7} \text{ cgs units}$$

The constant C of Eq 6 of Chapter 3 that is used for the calculation of the susceptibility of this sample at other temperatures is

$$C = \frac{\chi_T}{I_{v_T}} = \frac{-1\ 0540 \times 10^{-7}}{-0\ 17528}$$

$$= 6\ 0133 \times 10^{-7}$$

Therefore, the susceptibility at 101°K according to these data is

$$\chi_{101} = C I_{v_{101}}$$

$$= (6\ 0133 \times 10^{-7})\ (-0\ 18228)$$

$$= 1\ 0961 \times 10^{-7} \text{ cgs units}$$

In point of interest $H\ dH/dz$ may be calculated from these data if it is assumed that the force current response of the balance is 38 93 dynes/ma (cf sec 4 of chap 2)

$$H\frac{dH}{dz} = -\frac{\rho^*}{m}\frac{F_0^* - F_v^*}{\kappa_0^*} = -\frac{\rho^*}{m}(38\ 93)\frac{I_0^* - I_v^*}{\kappa_0^*}$$

$$= -\frac{5\ 3234 \times 38\ 93}{1\ 098}\ \frac{-0\ 21914 - (-0\ 17528)}{0\ 1404 \times 10^{-6}}$$

$$= 5\ 896 \times 10^7 \text{ gauss}^2/\text{cm}$$

2 ERRORS

The absolute calibration of the equipment is dependent upon the use of oxygen as a standard and therefore can be no more accurate than the value for the volume susceptibility of oxygen The uncertainty of the value ($0\ 1434 \times 10^{-6}$) is approximately 0 3% The pressure of the oxygen was maintained at 760 mm Hg as indicated by a calibrated manometer equipped with a vernier Errors from this source would be less than 0 03% The temperature of the gas at the time the calibration was made was known to within ±0 1°C and if a $1/T^2$ dependence of the volume susceptibility of oxygen is assumed an absolute error of less than 0 06% was contributed from this source The major uncertainty in the standardization was the purity of the oxygen According to the manufacturer s specifications the gas had an analysis of 99 5% oxygen 0 2% hydrogen and 0 3% nitrogen Prior to its being admitted to the pumped out susceptibility equipment the gas was passed over a palladium catalyst to burn out the hydrogen and through a solid carbon dioxide–acetone cold trap to remove the water The calibrating gas should have been 99 7% oxygen Analysis indicated only that its purity exceeded 99% Since the susceptibility of oxygen is higher by orders of magnitude than that of any gas other than nitric oxide the susceptibility of which is less than one half that of oxygen only the total oxygen present need be known Since exact knowledge of the analysis of the calibrating agent was not available no corrections for impurities in the standard have been made Therefore on an absolute basis the reported susceptibilities may be as much as 1 3% high or 0 3% low

Since the same source of gas the same purification train, and the same pressure and temperature measuring devices were used throughout this work the relative accuracy is not subject to the absolute uncertainties of the standard The precision of the data shall be considered from two points of

view (1) the determination of the room temperature susceptibilities of the samples and subsequent location of the χ vs T curves relative to each other and (2) the determination of lower temperature susceptibilities of a given sample relative to the room temperature value

The error in the location of the χ vs T curves relative to each other is primarily determined by the error in the quantity $(I_0^* - I_v^*)$ since I_0^* and I_v^* differ by approximately 25% In a typical determination I was measured under a given set of conditions with a precision of approximately ±0 04% exclusive of errors in the controlling conditions that is pressure field control pole face temperature, etc The latter effects were usually apparent and the errors contributed by them were found to be less than ±0 15% Furthermore, the effect of these errors was usually consistent throughout a given set of data (an example of the effect can be seen in the alternate sets of data for the low temperature portion of the curve for sample In 8 in Fig 12) Thus the total uncertainty in $(I_0^* - I_v^*)$ is ±0 6% and is the determining uncertainty in the placing of the curves relative to each other

The precision in the determination of the susceptibility of a sample as a function of temperature relative to its room temperature susceptibility is dependent upon the reproduction of conditions (field) the measurement of I upon setting the conditions and the measurement of the temperature The measurement of the temperature was found to be the least source of error in that the susceptibilities of the samples were found to change less than 0 05% per degree change in temperature Temperatures were measured with an accuracy of ±0 2°C Experiment indicated that with continuous operation the reproducibility of a given field was ±0 1% or better and was the main source of error in determining the χ vs T curves Upon reactivation of the equipment after an overnight shutdown reproducibility in the determination of a susceptibility at a given temperature was 0 15% Since in most cases the points determining a given curve were obtained in a continuous run the maximum relative error in the location of any point is ±0 1% In the general case the error is approximately ±0 05%

3 TABLES AND PLOTS OF DATA

Table 2 lists the germanium samples studied in this research, their type and carrier concentrations as determined from Hall coefficient data obtained by J W Cleland and the period of irradiation to which some of the specimens were subjected Table 3 is a tabulation of the results obtained by calculating the room-temperature susceptibility of each sample from I_0^* and I_v^* data obtained at five settings of the magnet controls For each sample the room temperature susceptibility was taken as the weighted average of the five values The average values are given in the seventh column of Table 3

Tables 4 and 5 are tabulations of the calculated susceptibilities at temperatures other than room

TABLE 2 CARRIER CONCENTRATIONS AT ROOM TEMPERATURE AND IRRADIATION TIME

PURDUE SPECIMEN NUMBER	BEFORE IRRADIATION		IRRADIATION TIME (hr)	AFTER IRRADIATION		CONCENTRATION OF TRAPPED CARRIERS (cm^{-3})
	Type of Ge m n um	Carrier Concentration (cm^{-3})		Type of German um	Carrier Concentration (cm^{-3})	
In-2B	p	$5\ 4 \times 10^{17}$	47	p	$4\ 5 \times 10^{7}$	9×10^{16}
In-8	p	$2\ 1 \times 10^{17}$				
ORB 78	p	$1\ 9 \times 10^{14}$				
ORD 7D	n	$1\ 3 \times 10^{14}$				
Sb-5A	n	$5\ 9 \times 10^{16}$	167	p	$8\ 0 \times 10^{16}$	$1\ 4 \times 10^{17}$
Sb-7	n	$1\ 3 \times 10^{18}$	118	$n-p$	$3\ 8 \times 10^{16}$	$1\ 3 \times 10^{18}$

temperature obtained by using the average values at room temperature as references in accordance with Eq 6 of Chapter 3 The data tabulated in Tables 4 and 5 are plotted in Figs 11 and 12

The letter I in the sample number indicates an irradiated specimen For instance In 2B and In 2B I are the same specimen, the latter number being used to designate the sample after irradiation

TABLE 3 ROOM-TEMPERATURE SUSCEPTIBILITY DETERMINED AT VARIOUS FIELDS

SAMPLE	ROOM TEMPERATURE SUSCEPTIBILITY ($-\chi \times 10^7$)						TEMPERATURE (°K)
	Field (kilogauss)					Average	
	1	13	15	18	21		
In 2B	1 058	1 057	1 059	1 058	1 059	1 058	292 9
In 2B I		1 048	1 054	1 057	1 054	1 054	295 2
In 8	1 048	1 048	1 049	1 046	1 053	1 048	297 3
ORB 78	1 073	1 067	1 058	1 061	1 060	1 060	294 4
ORD 7D	1 051	1 054	1 049	1 048	1 050	1 050	298 3
Sb 5A	1 051	1 051	1 057	1 061	1 058	1 056	292 9
Sb 5A I		1 054	1 057	1 054	1 054	1 054	296 3
Sb 7	1 054	1 059	1 053	1 053	1 051	1 053	297 3
Sb 7A	1 055	1 049	1 053	1 051	1 052	1 052	295 4

The letter I after the sample number indicates that the data were taken after irradiation of the s mple

TABLE 4 MAGNETIC SUSCEPTIBILITY VS TEMPERATURE FOR *n* TYPE GERMANIUM

ORD 7D		Sb 5A		Sb-5A I		Sb-7		Sb-7 I	
T (°K)	$-\chi \times 10^7$	T (°K)	$-\chi \times 10^7$	T (°K)	$-\chi \times 10^7$	T (°K)	$-\chi \times 10^7$	T (°K)	$-\chi \times 10^7$
298	1 0500	293	1 0560	296	1 0540	297	1 0528	295	1 0520
203	1 0715	201	1 0769	203	1 0750	203	1 0782	205	1 0747
166	1 0794	166	1 0846	166	1 0824	168	1 0857	167	1 0831
121	1 0881	121	1 0944	121	1 0925	121	1 0953	122	1 0928
101	1 0915	101	1 0981	101	1 0961	102	1 0982	101	1 0970
		88	1 1004	88	1 0984	86	1 1001		
			1 1014						
66	1 0957	69	1 1046	65	1 1013	84	1 1013	67	1 1023

Sample number

TABLE 5 MAGNETIC SUSCEPTIBILITY VS TEMPERATURE FOR *p* TYPE GERMANIUM

In 2B		In 2B I		In 8		ORB 78	
T (°K)	$-\chi \times 10^7$	T (°K)	$-\chi \times 10^7$	T (°K)	$-\chi \times 10^7$	T (°K)	$-\chi \times 10^7$
293	1 0580	295	1 0540	297	1 0480	294	1 0600
202	1 0805	205	1 0786			207	1 0789
167	1 0917	172	1 0878	186	1 0750		
				179	1 0784	164	1 0875
122	1 1064	124	1 1032	122	1 0918	122	1 0956
			1 1027	139	1 0886		
101	1 1144			101	1 0984	101	1 0993
88	1 1190	88	1 1146	89	1 1020	88	1 1010
				88	1 1027		
		79	1 1171	66	1 1088	66	1 1041
		72	1 119				

*Sample number

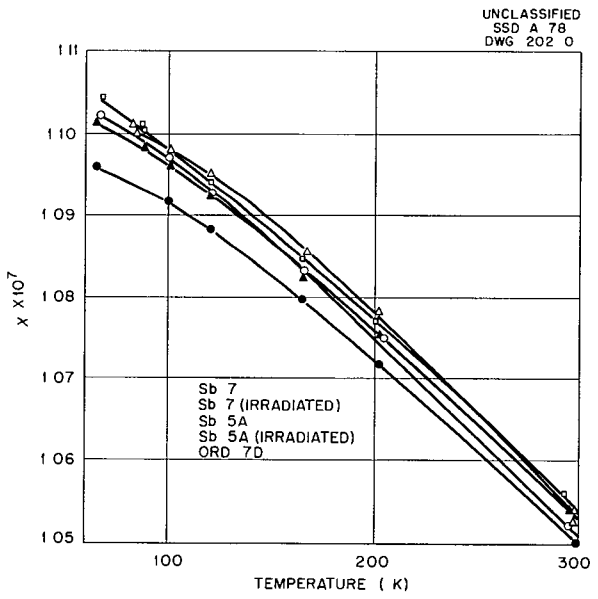

Fig 11 Magnetic Susceptibility of *n* Type Germanium Cubes

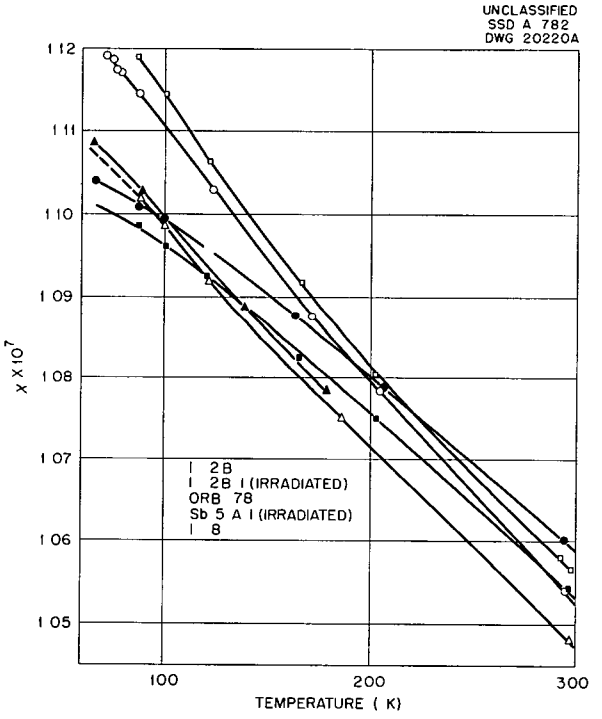

Fig 12 Magnetic Susceptibility of *p*-Type Germanium Cubes

CHAPTER 5 DISCUSSION OF RESULTS

1 GENERAL TEMPERATURE DEPENDENCE OF THE SUSCEPTIBILITY

It is readily apparent from the susceptibility vs temperature curves of Figs 11 and 12 that a common property is exhibited by all of the measured specimens there is a decrease in the diamagnetic susceptibility with increasing temperature Regardless of the nature of the curvature of the individual curves at low temperature they all appear to approach the same slope (~2 4 × 10^{-11} cgs units deg^{-1}) near room temperature Since this slope is a common property of all the curves, independent of the impurity content of the sample it may be assumed to be an intrinsic property of the host lattice exclusive of disorder impurities or carriers The slopes are listed in Table 6

TABLE 6 SLOPE OF χ VS T CURVES AT ROOM TEMPERATURE

SAMPLE	$\frac{\Delta\chi}{\Delta T} \times 10^{11}$
In 2B	2 56
In 2B I	2 60
In-8	2 43
ORB 78	2 47
ORD 7D	2 31
Sb-5A	2 29
Sb-5A I	2 31
Sb 7	2 53
Sb-7 I	2 47
Average	2 44 cgs u its deg^{-1}

The equation for the specific diamagnetic susceptibility of an assembly of spherically symmetrical atoms is given by

$$\chi = -\frac{N}{A}\frac{e^2}{6mc^2}\bar{r}^2 , \tag{1}$$

where N is Avogadro s number, A is the atomic weight c is the velocity of light e and m are the charge and mass of the electron respectively, and $\bar{r}^2$ is the mean square of the atomic radius If it is assumed that effects resulting from covalent binding may be disregarded and that the atoms may be regarded as spherically symmetrical Eq 1 yields for germanium

$$\chi = -8 \times 10^{-8} \text{ cgs units}$$

The only manner in which temperature may affect Eq 1 is through $\bar{r}^2$ Differentiating Eq 1 logarithmically with respect to temperature gives

$$\frac{1}{\chi}\frac{d\chi}{dT} = \frac{1}{\bar{r}^2}\frac{d\bar{r}^2}{dT} , \tag{2}$$

the right hand term of which is equal to ⅔ the coefficient of cubical expansion α which for germanium is 18 × 10^{-6} deg^{-1} Hence

$$\frac{1}{\chi}\frac{d\chi}{dT} = 1\ 2 \times 10^{-5}$$

which is smaller by a factor of approximately 20 than the observed relative temperature variation

$$-\frac{2\ 4 \times 10^{-11}}{1\ 05 \times 10^{-7}} = -2\ 3 \times 10^{-4} \text{ deg}^{-1}$$

It is to be noted, also, that the variation is in the wrong direction since by Eq 2 the diamagnetism should decrease with decreasing temperature

There appears to be no theory available to explain this behavior The Peierls[34] theory is not applicable to solids with completely filled energy bands such as those under discussion A similar temperature dependence of the diamagnetism of gray tin was not considered by Busch and Mooser[9] when determining the contribution of the intrinsic carriers If such an effect exists in gray tin and if it were not accounted for, its neglect would lead to a smaller apparent forbidden gap width because of an apparently smaller temperature dependence of the carrier concentrations

A second general conclusion which may be drawn from an inspection of Figs 11 and 12 is the complete absence of a sharp increase in the diamagnetic susceptibility of germanium at 75°K [45] a temperature at which Simon and Cristescu[14] found an anomaly in the specific heat curve Subsequent measurements of the specific heat[16] have failed to confirm Simon and Cristescu's unexplained results In this work the susceptibilities of seven samples were measured at temperatures

below 75°K (as low as 65°K in one instance) and no indications of deviations from smooth curves were detected There appears to be no theoretical basis for expecting the reported anomaly

2 IMPURITY AND CARRIER CONTRIBUTIONS

2 1 Estimate of the Effect Before attempting to analyze the results further it would be desirable to check the limit of applicability of the equipment for detecting contributions to the susceptibility of the charge carriers The magnitude of the contri bution may be calculated from Eqs 14 and 15 of Chapter 1 by which the susceptibility for carriers is

$$\chi_c = \frac{\beta^2 n_z}{3\rho kT} (3 - f_z^2) \tag{3}$$

The results of such calculations for various as sumed values of the freedom number f_z at 300 and 100°K for germanium with a carrier concentration $n_z = 10^{18}$ cm^{-3} are

f_z	χ_c (cgs units) At 300°K	At 100°K
0 25	$3\ 9 \times 10^{-10}$	$1\ 2 \times 10^{-9}$
1 0	$2\ 6 \times 10^{-10}$	$7\ 8 \times 10^{-10}$
$\sqrt{3}$	0	0
2 0	$-1\ 3 \times 10^{-10}$	$-3\ 9 \times 10^{-10}$
4 0	$-1\ 7 \times 10^{-9}$	$-5\ 1 \times 10^{-9}$

Since the relative precision of the χ vs T points for any sample is approximately 0 1% it is evident that it would be possible to detect the effect of carriers on the χ vs T plots except when the freedom number approached $\sqrt{3}$ However because of the lower precision in locating the curves relative to each other (cf sec 3 of chap 4) it is not possible to determine by subtraction absolute differences in the carrier contribution from speci men to specimen with any degree of precision It is evident that the value of the freedom number plays an important role in the magnitude of the carrier contribution For $f_z = \sqrt{3}$, no contribution would be observed

Figures 13 and 14 are plots vs $1/T$ of the point by point differences of the χ vs T curves for n and p type material The choice of ORD 7D as the reference curve for n type germanium and ORB 78 for the p type germanium will be explained below The precision indicated on each figure is the relative precision which is of interest when the slopes of these curves are studied As explained above the absolute accuracy is lower by a factor of approximately 6 and as a result, the values of $\Delta\chi$ considered individually are of questionable worth However it will be shown that the slopes are of great interest and therefore they are listed in Table 7

2 2 *p* Type Germanium The susceptibility vs temperature curves for p type germanium are shown in Fig 12 The purest specimen (ORB 78), whose hole concentration is approximately $1\ 9 \times 10^{14}$

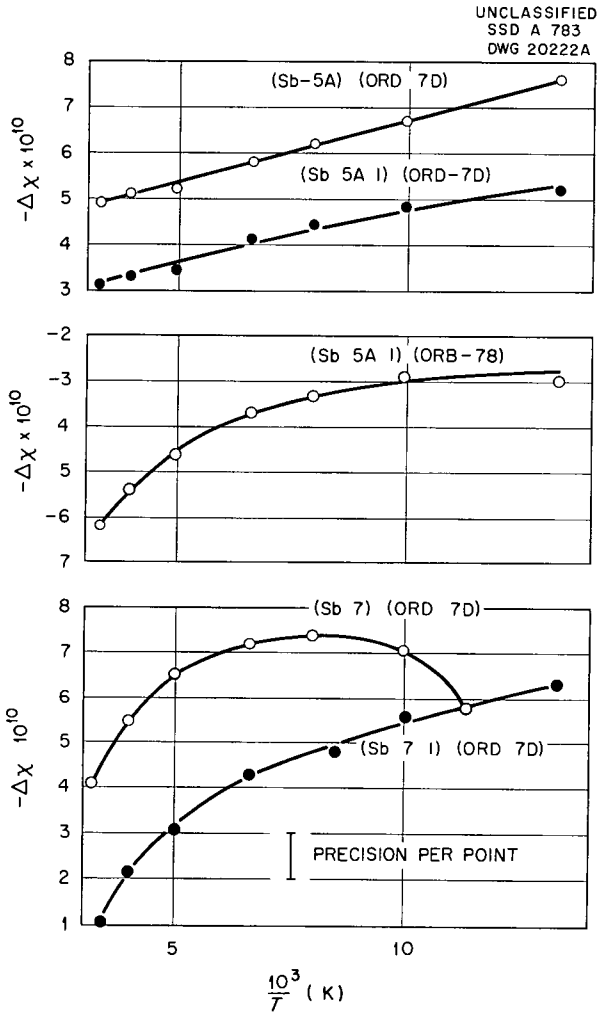

Fig 13 $\Delta\chi$ vs $1/T$ of n Type Germanium

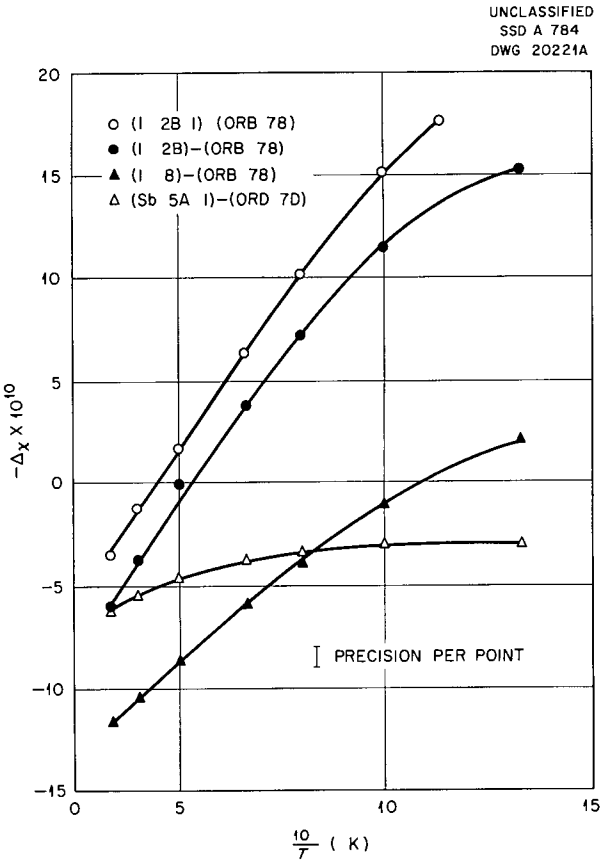

Fig 14 $\Delta\chi$ vs $1/T$ of p Type Germanium

TABLE 7 SLOPE OF $\Delta\chi$ VS $1/T$ CURVES AT ROOM TEMPERATURE

CURVE	$\frac{\Delta(\Delta\chi)}{\Delta(1/T)}$	$\frac{\Delta(\Delta\chi)}{\Delta(1/T)} \frac{3\rho k}{\beta^2}$
(Sb 5A)-(ORD 7D)	$-2\ 2 \times 10^{-8}$	$-5\ 6 \times 10^{17}$
(Sb-5A I)-(ORD 7D)	$-2\ 4 \times 10^{-8}$	$-6\ 1 \times 10^{17}$
(In 2B I)-(ORB-78)	$-2\ 9 \times 10^{-7}$	$-7\ 4 \times 10^{18}$
(I 2B)-(ORB 78)	$-3\ 0 \times 10^{-7}$	$-7\ 7 \times 10^{18}$
(In 8)-(ORB 78)	$-1\ 8 \times 10^{-7}$	$-4\ 6 \times 10^{18}$

cm^{-3} yields a curve which (1) is concave downward whereas the curves of the more impure specimens (In 8 In 2B, In 2B I) exhibit an upward curvature, and (2) is essentially parallel to the curve for the high purity n type specimen (ORD 7D) If it is assumed that the impurity and the carrier contributions to the susceptibility of ORB 78 are negligible (according to Eq 3 a freedom number of approximately 100 would be required to make the carrier contribution $\chi_c = -10^{-10}$) the susceptibility vs temperature curve of this sample may be taken as that of the pure material Upon subtracting this curve point by point from that of a more impure sample, the sum of the unionized impurity and the carrier contributions should be obtained These contributions represented as excess diamagnetism ($-\Delta\chi$) are plotted as a function of reciprocal absolute temperature in Fig 14 The results are given for unirradiated specimens In 8 and In 2B and in addition for irradiated specimens In 2B I and Sb 5A I the latter being converted from n to p type by bombardment The carrier concentrations and bombardment histories of these samples are given in Table 2 It is obvious in every case shown in Fig 12 that the sum of the impurity and carrier contributions is diamagnetic The sum as given by Eqs 13 14, and 15 of Chapter 1 is

$$(4) \qquad \Delta\chi = \chi_{I,c} = \frac{\beta^2}{3\rho kT} (3N_A - n_b f_b^2)$$

The derivative of this equation with respect to $1/T$ if f_b is assumed temperature independent gives the relation

$$(5) \qquad \frac{d(\Delta\chi)}{d\frac{1}{T}} = \frac{d\chi_{I\,c}}{d\frac{1}{T}}$$

$$= \frac{\beta^2}{3\rho k} \left[(3N_A - n_b f_b^2) - \frac{f_b^2}{T} \frac{dn_b}{d\frac{1}{T}} \right]$$

The data reveal that $n_b f_b^2 > 3N_A$ and causes the first term inside the brackets to be negative Since $dn_b/d(1/T)$ is always negative the absolute value of the slope should decrease in magnitude with increasing $1/T$ This behavior is borne out by the data

The freedom number for the holes f_b, has been calculated for the In" series of samples by using Eq 5, and the results are tabulated in Table 8 Because of the large relative error involved in this calculation the values are probably not accurate to better than approximately 50% Also listed in Table 8 are the other necessary parameters [n_b,

TABLE 8 CALCULATED FREEDOM NUMBER OF HOLES IN GERMANIUM

SAMPLE	$1/T$	n_b	$dn_b/d(1/T)$*	N_A	$\frac{d(\Delta\chi)}{d(1/T)}$	f_b
In 2B	$3\ 5 \times 10^{-3}$	$5\ 35 \times 10^{17}$	$-5\ 6 \times 10^{19}$	8×10^{17}	$-3\ 0 \times 10^{-7}$	5 5
In 2B I	$3\ 5 \times 10^{-3}$	$4\ 4 \times 10^{17}$	-6×10^{19}	7×10^{17}	$-2\ 9 \times 10^{-7}$	6 4
In 8	$3\ 5 \times 10^{-3}$	$2\ 06 \times 10^{17}$	$-2\ 2 \times 10^{19}$	3×10^{17}	$-1\ 8 \times 10^{-7}$	6 5

These v lue were calculated from Hall coefficient data obtained on compa ion crystals by J W Cleland

$dn_b/d(1/T)$ N_A and $d(\Delta\chi)/d(1/T)$] obtained from Hall coefficient data and the $\Delta\chi$ vs $1/T$ curve

2 3 *n* Type Germanium The χ vs T curves for *n* type germanium are shown in Fig 11 In contrast to the *p* type curves all show a concave downward curvature Sample ORD 7D is a high purity ($n_e \sim 10^{14}$) *n* type sample and the curvature of its $-\Delta\chi$ vs T plot is practically identical with that of ORB 78 Sample Sb 5A has an electron concen tration at room temperature of $5\ 6 \times 10^{16}$ cm^{-3} and in this case, calculations of impurity and carrier contributions would indicate that, even under favorable conditions of freedom number and temper ature, the carrier contribution to the susceptibility would be of the same order of magnitude as the experimental uncertainty Hall coefficient measure ments on sample Sb 7 indicate a carrier concen tration of about 10^{18} However the behavior of the resistivity of the monitoring crystal during bombardment indicates a rather large anomaly and the carrier concentration of the susceptibility cube may be lower by an order of magnitude This may be the reason why no contribution was observed for this specimen

The $-\Delta\chi$ vs $1/T$ curves for the *n* type suscepti bilities (Fig 13) were constructed by subtracting the values for ORD 7D at different temperatures from the values for the more impure specimens in the same manner as for *p* type germanium It should be noted that the experimental uncertainty (1×10^{-10} cgs units) is an appreciable portion of the over all temperature variation Therefore no attempt has been made to make detailed calculations of f_e except for Sb 5A In this case, it was found that $f_e \sim 4$ which is probably not more reliable than an order of magnitude

It was pointed out above that Sb 7 was an anomal ous sample The $-\Delta\chi$ vs $1/T$ curve for this sample also shows a strange curvature but because of the large uncertainty of the $\Delta\chi$ values, this is probably not significant

It should also be kept in mind that if $f_e = \sqrt{3}$ any contribution of the impurities and carriers to the susceptibility would be small since $N_D \cong n_e$ However the mobility of electrons is larger than that of holes in germanium which indicates that $f_e > f_b$ In view of the large value of f_b obtained in the preceding section the possibility that $f_e = \sqrt{3}$ does not appear likely

3 IRRADIATION

The results of irradiation appear to be incon clusive primarily because an insufficient number of samples was studied The slopes of the high temperature portions of the χ vs T curves appear to be unaltered by irradiation The arguments set forth in previous sections of this chapter lead to the conclusion that the temperature dependence of the host lattice is not appreciably altered by irradiation A more conclusive statement would require data taken at a higher temperature since the curves appear to approach parallelism just below room temperature

What appears to be an effect of irradiation is evident in the low temperature portion of the In 2B curves, Figs 12 and 14 There is a smaller in crease in the diamagnetic susceptibility at low temperatures in the irradiated case as compared with the unirradiated case This is to be expected, since conductivity and Hall studies of irradiated germanium[13] indicate an increase in the activation energy of holes upon irradiation

The anticipated radiation effects on the magnetic susceptibility of Sb 7 were not observed However the anomalous behavior of the companion monitoring crystal and the appearance of the $-\Delta\chi$ vs $1/T$ curve would indicate that the sample was not homogeneous and thus not representative of *n* type germanium According to the arguments set forth in Section 2 1 of this chapter if the electron concentration of sample Sb 7 were lower by a factor of 10 than the assumed concentration, the effect would fall within the uncertainty of the experimental measurements By the same token, the assumed electron concentration of sample Sb 5 is not sufficiently great to cause a detectable effect

Samples with a higher carrier concentration subjected to longer periods of irradiation are necessary for a more definitive study of the effect of fast neutron bombardment

---

CHAPTER 6 SUMMARY AND CONCLUSIONS

A balance was designed and constructed that had sufficient sensitivity and precision to measure differential forces of 10^{-3} to 10^{-4} dynes in the presence of 1000 dyne forces exerted in the same direction

Accessory equipment for the measurement of the magnetic susceptibility of germanium was also assembled

The magnetic susceptibilities of six annealed and three fast neutron bombarded single crystal cubes of germanium were measured as functions of temperatures from liquid nitrogen temperatures to room temperature

High purity germanium has a diamagnetic susceptibility of $(1\ 05 \pm 0\ 01) \times 10^{-7}$ at room temperature

The diamagnetic susceptibility of the germanium lattice is temperature dependent it decreases linearly with increasing temperature in the room temperature range The average slope of the nine samples studied is

$$\frac{\Delta\chi}{\Delta T} = 2\ 44 \times 10^{-11} \text{ cgs units deg}^{-1}$$

The anomalous behavior of the susceptibility at 75°K as reported by Squire was not observed in any of the samples studied

The contributions of the unionized impurities and of the current carriers to the susceptibility were detected in the case of *p* type germanium the contributions were diamagnetic at liquid nitrogen temperatures The freedom number for holes appeared to be of the order of 6 in the cases studied

The detection of the contributions of the unionized impurities and of the current carriers to the susceptibility of *n* type germanium is questionable although the contributions appeared to be diamagnetic

The effect of fast neutron bombardment was detected in one *p* type sample Relative to the unirradiated specimen the effect was that of decreased diamagnetism at low temperature and was in accord with predicted results from Hall coefficient and electrical conductivity studies

The radiation effect was not detected in *n* type samples presumably because of insufficient concentration of carriers and suspected inhomogeneity Therefore the nature of the radiation produced electron traps was not discernible These results indicate that further work in this field would require the use of *n* type specimens with higher carrier concentration and of longer periods of irradiation

BIBLIOGRAPHY

1 Almen J O *Pretwisted Torsion Plate Spring* U S Patent 2 238,380 (April 15, 1941)

2 Bates L F *Modern Magnetism* 3d ed Cambridge University Press Cambridge, 1951

3 Blewitt T H and Coltman, R R The Effect of Pile Irradiation on the Stress Strain Curve of Copper *Phys Rev* **82** 769 (1951)

4 Blewitt T H, and Coltman R R The Effect of Neutron Irradiation on Metallic Diffusion *Phys Rev* **85** 384 (1952)

5 Billington D S and Siegel, S Effect of Nuclear Radiation on Metals *Metal Prog* **58** 847 (1950)

6 Bitter F On the Magnetic Properties of Metals *Phys Rev* **36** 978 (1930)

7 Bitter F and Reed F E A New Type of Electromagnet Part I Operation at 20-kw Level *Rev Sci Instr* **22** 171 (1951)

8 Bozorth, R M, *Ferromagnetism* Van Nostrand New York 1951

9 Busch G and Mooser E Magnetische Suszeptibilitat des grauen Zinns *Z physik Chem* **198** 23 29 (1951)

10 Cleland J W Billington D S and Crawford J H Jr, Low Temperature Fast Neutron Bombardment of Copper Beryllium Alloy *Bull Am Phys Soc* **28** (No 2) 40 (1953)

11 Cleland J W Crawford J H Jr Lark Horovitz K Pigg J C and Young F W Jr The Effect of Fast Neutron Bombardment on the Electrical Properties of Germanium *Phys Rev* **83** 312 (1951)

12 Collet P and Foex G Proprietes Magnetiques du Platine Differentes Varietes Influence du Champ Passage d un Etat a un Autre *J phys radium* **2** (Part 1) 290 (1931)

13 Crawford J H and Cleland J W Energy Level in Ge produced by Nucleon Bombardment *Phys Rev* **86** 641 (1952)

14 Cristescu S and Simon F, Die spezifischen Warmen von Beryllium Germanium und Hafnium bei tiefen Temperaturen *Z physik Chem* **25B** 273 (1934)

15 Donoghue, J J *An Apparatus for the Precise Measurement of Magnetic Susceptibilities by the Faraday Method* NAA SR 117 (May 25 1953)

16 Estermann I and Weertman J R, Effect of Impurity Content on the Specific Heat of Germanium ' *Phys Rev* **83** 228 (1951)

17 Fowler R H *Statistical Mechanics The Theory of the Properties of Matter in Equilibrium* Cambridge University Press Cambridge 1936

18 Hintenberger H Über die elektrischen Eigenschaften des Bleisulfids *Z Physik* **119**, 1 (1942)

19 Hodgman C D (ed) *Handbook of Chemistry and Physics*, 33 ed Chemical Rubber Pub Co, Cleveland 1951

20 Honda K, and Shimizu Y The Effect of Cold Working on the Magnetic Susceptibility of Metals ' *Science Reps Tohoku Imp Univ First Ser* **20** 460 (1931)

21 Hutchison T S and Reekie J An Electrodynamic Balance for the Measurement of Magnetic Susceptibilities *J Sci Instr* **23** 209 (1946)

22 James H M and Lark Horovitz K Localized Electronic States in Bombarded Semiconductors " *Z physik Chem* **198** 107 (1951)

23 Klontz E E and Lark Horovitz K Electron Bombardment of Ge *Phys Rev* **82** 763 (1951)

24 Landau L, Diamagnetismus der Metalle," *Z Physik* **64** 629 (1930)

25 Lark Horovitz, K, Nucleon bombarded Semi conductors p 47 in *Semi Conducting Materials* ed by H K Henisch Butterworths Scientific Publications London 1951

26 McGuire T R and Lane C T Magnetic Susceptibility Balance for Use at Liquid Helium Temperatures *Rev Sci Instr* **20** 489 (1949)

27 Mott, N F and Gurney R W, *Electronic Processes in Ionic Crystals* Clarendon Press Oxford 1940

28 Murray G T and Taylor W E *Effect of Neutron Irradiation on Supersaturated Solid Solution of Beryllium in Copper* ORNL 1323 (Jan 30 1953)

29 Nelson C M *Magnetochemistry of Technetium and Rhenium* unpublished Ph D Dissertation, University of Tennessee 1952

30 Nelson, C M Sproull R L, and Caswell R S, Conductivity Changes in KCl Produced by γ and n Irradiation ' *Phys Rev* **90**, 364 (1953)

31 Osborne M F M Number Theory and the Magnetic Properties of an Electron Gas " *Phys Rev* **88** 438 (1952)

32 Owen M Magnetochemische Untersuchungen Die thermomagnetischen Eigenschaften der Elemente *Ann Physik* **37** 657 (1912)

33 Pauli W Jr Uber Gasentartung und Paramagnetismus *Z Physik* **41** 81 (1927)

34 Peierls R Zur Theorie des Diamagnetismus von Leitungselektronen " *Z Physik* **80** 763 (1933)

35 Pigg J C Field Control for the ADL Magnet, *Solid State Division Quarterly Progress Report for Period Ending February 10 1953* ORNL 1506 p 49

36 Pigg J C Cleland J W Crawford J H and Lark Horovitz K Pile Irradiation of Semiconducting Cu_2O *Phys Rev* **82** 763 (1951)

37 Ramachandra Rao, S Magnetism of Germanium ' *Current Sci (India)* **14** 19 (1945)

38 Roters H C *Electromagnetic Devices* Wiley New York 1941

39 Seitz F On the Disordering of Solids by Action of Fast Massive Particles *Discussions Faraday Soc* **5** 271 (1949)

40 Seitz F *The Modern Theory of Solids* McGraw Hill New York 1940

41 Selwood P W *Magnetochemistry* Interscience New York 1943

42 Slater J C The Effects of Radiation on Materials,' *J Appl Phys* **22** 237 (1951)

43 Smith A L and Johnson H L *The Magnetic Susceptibility of Liquid Nitric Oxide and the Heat of Dissociation of $(NO)_2$ A Cryostat for Susceptibility Measurements,* Ohio State TR 328-15 (Dec 15 1951)

44 Sondheimer E H and Wilson A H, The Diamagnetism of Free Electrons ' *Proc Roy Soc (London)* **210** 173 (1951)

45 Squire C F Abnormal Diamagnetism of Ge at Low Temperatures the Specific Heat of Zr, ' *Phys Rev* **58** 202 (1940)

46 Steele M C, Application of the Theory of Numbers to the Magnetic Properties of a Free Electron Gas, *Phys Rev* **88** 451 (1952)

47 Stöhr V H and Klemn W Uber Zweistoffsysteme mit Germanium II, *Z anorg u allgem Chem* **244** 205 (1940)

48 Stoner E C The Temperature Dependence of Free Electron Susceptibility *Proc Roy Soc (London)* **152A** 672 (1935)

49 Straumanis M E and Aka E Z Lattice Parameters Coefficients of Thermal Expansion and Atomic Weights of Purest Silicon and Germanium " *J Appl Phys* **23** 330 (1952)

50 Strong, J *et al* *Procedures in Experimental Physics* Prentice-Hall New York, 1938

51 Teller E Der Diamagnetismus von freien Elektronen ' *Z Physik* **67** 311 (1931)

52 Van Vleck J H *The Theory of Electric and Magnetic Susceptibilities* Clarendon Press Oxford 1932

53 Waindle R F New Uses for Cobalt Base Spring Alloy *Metal Progr* **56** 808 (1949)

54 Wittels M C, The Lattice Expansion of Quartz Due to Fast Neutron Bombardment ' *Phys Rev* **89** 656 (1953)